REFLECTION IMAGE OF THE EASTERN MONTSERRAT CRUST, MONTSERRAT, WEST INDIES

By

David Bradly Christensen

A thesis submitted in partial fulfillment

of the requirements for the

Masters of Science Degree in Geophysics

Department of Earth and Environmental Science

Graduate College

New Mexico Institute of Mining and Technology

December 2009

ABSTRACT

In order to better understand crustal structure of the Lesser Antilles arc and its relationship to the evolution of volcanic centers, the onshore-offshore SEA-CALIPSO seismic imaging experiment was conducted in December 2007. Over 200 seismometers on-land and offshore recorded data from airguns towed by the RSS James Cook. We analyzed a subset of data from the 4.5 km Silver Hills profile of single component seismometers in northern Montserrat, using several seismic reflection stacks located off the east coast. We identified two reflectors, a mid-crustal reflector, and the Moho, identified at about 9 s twt, corresponding to a depth of 23 km. The mid-crustal reflector indicates a crustal boundary at ~5 s twt (corresponding to a depth of ~12 km) with an upper layer of intermediate composition and velocities of 6.0-6.3 km/s, and a lower mafic layer with velocities of 6.9-7.0 km/s. This reflector suggests the crust near Montserrat maybe undergoing compositional changes towards a more felsic material. By showing an intermediate composition, this reflector indicates that island arcs are an important part of crustal evolution and facilitate the creation of felsic crust. This suggests that there maybe more felsic material within the subduction zone complex than previously thought, similar to that of Isu-Bonin or the South Sandwich Islands.

ACKNOWLEDGMENTS

Many thanks to the SEA-CALIPSO team for acquiring and providing these data for processing. Thanks to my committee Drs. Susan Bilek, Kent Condie, and especially my advisor Dr. Catherine Snelson who endured many hours of editing, and complaining. Thanks to Sandra Saldana for talking me off the ceiling when things went wrong, and for the support and friendship that got me through graduate school. Thanks to Dana Hackney the "ProMAX guy" who answered many questions on processing and debugged my flows. Thanks to Pam Moyer, Matthew Earthman and Leigh Davidson who read early manuscripts of my proposal, which eventually became this thesis. Thanks to Jonathan MacCarthy for his GMT expertise. Thanks to Barry Voight for organizing a special publication in GRL. Thanks to Jaron Ross for his assistance on formatting. Thanks to Shari Houston, Matthew Earthman, and Natalie Earthman for true friendship and "Lost" nights. Thanks to IRIS PASSCAL for instruments and technical support for the SEA-CALIPSO experiment. Thanks to the National Science Foundation for their grant that provided funds for the SEA-CALIPSO experiment. Special thanks to my parents, Bruce and Nancy Christensen, for teaching me how to believe in myself and to work hard to accomplish my goals.

TABLE OF CONTENTS

LIST OF FIGURES

LIST OF TABLES

This thesis is accepted on behalf of the
Faculty of the Institute by the following committee:

Catherine M. Snelson, Advisor

Susan L. Bilek

Kent C. Condie

Date

I release this document to the New Mexico Institute of Mining and Technology.

D. Bradly Christensen Date

CHAPTER 1 INTRODUCTION

Despite several previous studies (MacGregor, 1938; Boynton et al., 1979; Baker, 1984) and numerous recent investigations of Montserrat that were stimulated by the eruption of the Soufriere Hills volcano (Druitt and Kokelaar, 2002), the structure of the arc crust and volcanic system of Montserrat remained poorly understood (Macdonald et al., 2000). In an effort to improve basic understanding, the onshore-offshore SEA-CALIPSO (Seismic Experiment with Airgun-source – Caribbean Andesitic Lava Island Precision Seismo-geodetic Observatory) seismic refraction/reflection experiment was conducted in December 2007 [Voight et al., in review 2009]. The experiment used an airgun source from the RRS James Cook, and recorded seismic energy on a dense seismometer network on the island and also on ocean-bottom seismometers arrayed offshore [Paulatto et al., in press, 2009].

This paper presents and evaluates seismic reflection data acquired in the northern part of Montserrat. We examine ship-track segments corresponding to quasi-linear arrays of single-component seismic recorders, and a subset of data from the Centre Hills-to-Silver Hills profile is chosen for detailed processing (Fig. 1). We identify several crustal reflectors and test four hypothetical crustal models to explain the data. Our preferred model has a crust composed of an upper layer of fractured felsic-intermediate composition with velocities of 6.0-6.3 km/s underlain at ~5 s two-way travel-time (twt)

by a mafic layer with velocities of 6.9-7.0 km/s. The Moho is also identified at about 9 s twt.

Figure 1: Montserrat is located on the eastern edge the Caribbean plate (inset). The SEA-CALIPSO experiment included: 4402 airgun shots, dotted line; 10 Montserrat Volcano Observatory instruments (MVO), diamonds; 28 RT130 3 component record ers, circles; and 202 RT125a single channel record ers (Texans), triangles. The Silver Hills profile (SHP) runs north to south, the Centre Hills profile (CHP) runs west to east, the Garibaldi profile (GP) runs southwest to northeast and the Belham Valley profile (BVP) runs from northwest to southeast, radial to Soufriere Hills volcano. Location of imaged crust, (SH 540 stack, SH 550 stack, and SH 560 stack), and shots (SH 540, SH 550, SH 560) are shown.

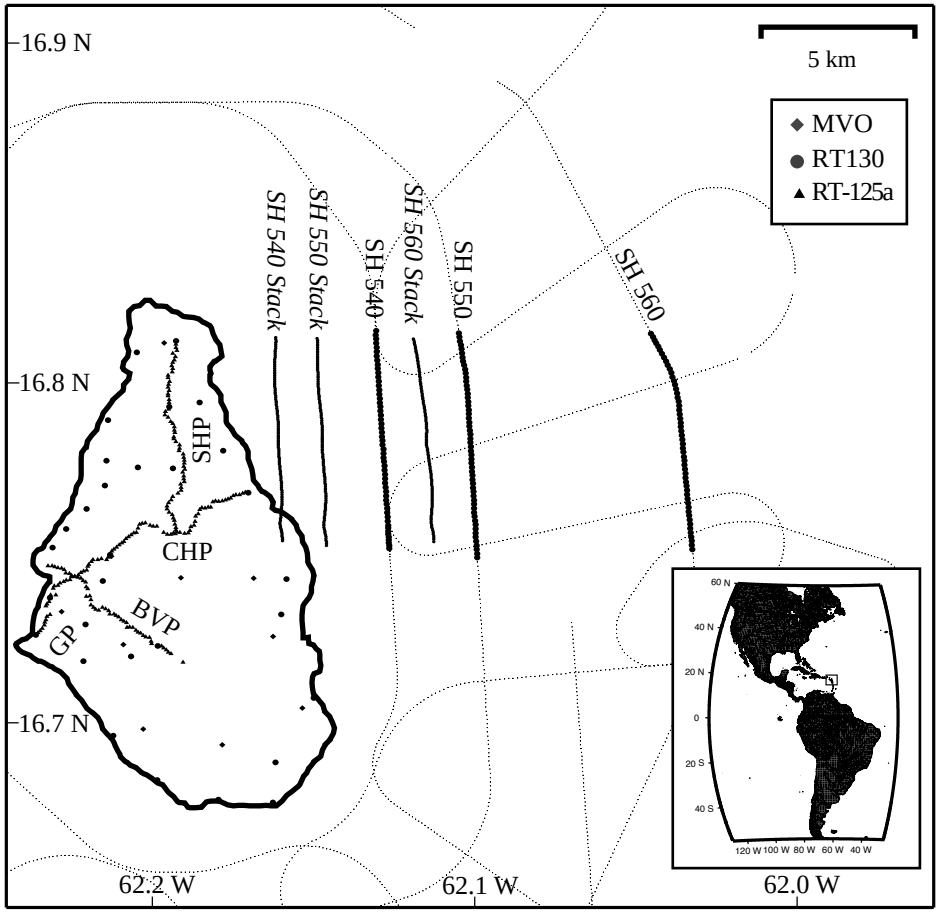

CHAPTER 2 GEOLOGICAL AND GEOPHYSICAL SETTING

A complete discussion of the geologic and geophysical background of the Caribbean and Montserrat can be found in Appendix A and B respectively.

Montserrat is located at the northern end of the Lesser Antilles island arc, which has resulted from subduction of the North American plate beneath the Caribbean plate at a rate of 2 cm/a (e.g., Druitt and Kokelaar, 2002). The northern arc volcanoes are founded on a Cretaceous oceanic island arc (Bouysse and Guennoc, 1983; Bouysse and Westercamp, 1990). The structure of this arc consists of the Atlantic oceanic crust; the forearc; the Lesser Antilles; and the Grenada Basin which lies behind the arc (e.g., Wadge, 1994). Formation of the volcanic islands initiated in the Miocene when the axis of the northern arc migrated westwards at ~23 Ma (e.g., Pindell, 1994). The crust has a thickness of about 30 km or less [Boynton, et al., 1979; Case et al., 1984; Sevilla et al., manuscript in review, 2009]. The plate interface dips at a shallow angle west of the trench and much more steeply (50-60^{o}) under the arc, with a flexure offshore the outer islands (Feuillet et al., 2002, Fig. 2). The asthenosphere wedge is around 100 km deep (Bouysse and Westercamp, 1990).

The subaerial part of Montserrat is 16 km N-S by 9 km E-W and is made almost exclusively of volcanic rocks, bordered by a shallow (< 100 m) marine shelf 14 km x 18 km in extent [Sevilla et al., manuscript in review, 2009]. Montserrat caps a compound

volcanic edifice that extends from about 1000 m asl, to 700-900 m bsl, where the basal dimensions are about 30 km N-S) and 15-25 km E-W [Sevilla et al., manuscript in review, 2009]. There are three volcanic massifs, from north to south, Silver Hills (SH, c. 2.6-1.2 Ma), Centre Hills (CH, c. 0.95-0.55 Ma), and Soufriere Hills – South Soufriere Hills (SHV-SSH) (c. 0.3 Ma-present) (e.g., Kokelaar, 2002; Herd et al., 2005). Soufriere Hills Volcano has been active since 1995 (e.g., Kokelaar, 2002).

Previous geophysical studies of the Caribbean plate include gravity, seismic reflection/refraction, geodetic measurements and volcano-tectonic seismic studies (e.g., Officer et al., 1957; Boynton et al., 1979; Wadge, 1994; Neuberg et al., 1998; White et al., 1998; Voight et al., 2006; Christeson et al., 2008; Magnani et al., 2009). The remaining discussion is summarized in Boynton et al. (1979). An important large scale seismic refraction project (Lesser Antilles Seismic Project, or LASP) was carried out in 1972 to examine the crustal structure along the arc from Guadaloupe to Grenada, another line ran along the Aves Ridge, and a third line crossed the arc at the latitude of Barbados. Three crustal layers were found along the arc axis. The uppermost layer, 1-5 km thick, comprises lavas, pyroclastic deposits and marine sediments. The second has a thickness from 2 to 20 km (6-10 km thick under Dominica and Guadaloupe) and an average velocity of 6.2 km/s, suggesting dominance by plutonic rocks of intermediate composition. Poisson ratio was estimated from study of S and P waves as 0.26-0.27, typical of plutonic rocks and suggesting negligible fraction of magma in the second layer. The substantial relief of the surface of the second layer, rising between islands, suggested reinforcement of existing volcanic centers by repeated intrusions, rather than formation of new ones. The third and lowermost crustal layer, with average velocity 6.9 km/s, was

interpreted as of mafic composition, i.e. layer 3 oceanic crust on which the arc was formed and gabbros and cumulates remaining in magma chambers associated with arc volcanism.

Variations in layer velocity under Montserrat are reported by Sevilla et al. (this in review 2009). Moho depths were roughly estimated by Boynton et al. (1979), varying from about 23 km near St. Vincent to 30 km under Martinique (Boynton et al., 1979). Sevilla et al. (manuscript in review, 2009) report Moho depths around 28-30 km near Montserrat.

CHAPTER 3 DATA ACQUISITION

Shot and receiver locations are found in Appendix C.

In the SEA-CALIPSO experiment, 202 single channel seismic recorders (RT125a - Texans) and 28 3-component RT130s were installed on the island, supplementing 10 Montserrat Volcano Observatory (MVO) stations, and 10 Ocean Bottom Seismometers (OBS) that were emplaced offshore (Fig. 1). The single channel seismic recorders were placed in four profiles, with instruments spaced at ~100 m intervals. The so-called "Silver Hills profile" (SHP) runs northward from the Centre Hills to the Silver Hills, with 63 stations; the "Centre Hills profile" (CHP) crosses from west to east in mid-island, with 51 stations; the "Garibaldi profile" (GP) extends the Centre Hills line farther to the southwest, with 36 stations; and the "Belham Valley profile" (BVP) runs from northwest to southeast, radial to SHV, with 52 stations (Fig. 1). The Ocean Bottom Seismometers were placed west and south of the island while the Montserrat Volcano Observatory stations encircle the SHV. RT130s were placed around the island, to provide a gridded pattern where possible [Shalev et al., in review 2009; Voight et al., in review 2009]. An 8-airgun array with a total volume of 2600 cubic inches and a fired pressure of 2000 psi was towed by the RSS James Cook along transects around the island, providing 4402 shots at a spacing of ~130 m (Fig. 1). Overall, the seismic reflection data quality is good to poor; this was due to the volcanic nature of the island, lack of penetration of the

seismic energy, and lack of fold [cf. Paulatto et al., in review 2009]. Analyses of the shot location files reveal 36 lines that corresponded to source lines where the ship was nominally parallel with the instruments on the island. The SHP were chosen for processing, because they form three complete seismic reflection common midpoint (CMP) profiles in a compact region off the eastern coast of Montserrat and show reflections related to the Moho.

CHAPTER 4 PROCESSING

A complete discussion of processing is found in Appendix D.

In addition to the standard seismic reflection processing, because of relatively poor data quality, several multiple suppression filtering and migration schemes were conducted to improve the coherence of the seismic signal.

Processing steps for the SHP included top muting and trace editing to remove noisy traces; use of an automatic gain control (AGC) to adjust amplitudes; an elevation static shift to move the datum to sea-level; deconvolution to remove multiples; development of an interval velocity model based on published data; the application of the normal move-out (NMO); use of a Butterworth bandpass filter; and a zero-offset mean stack (Table 1) (e.g., Yilmaz, 2001). Velocity semblance was conducted for the Silver Hills data, which was unsuccessful. Instead data from seismic refraction/reflection experiments in the Caribbean area to develop an interval velocity model (Boynton et al., 1979; Christeson et al., 2008).

Additional processing were attempted, for multiple suppression and identifying refracted arrivals at the long offsets. These steps, detailed below, were unsuccessful.

Due to the geometry of the experiment, the typical near source arrival data were not obtained (Fig. 1). As a result, the SHP data are located at offsets where the reflected and refracted arrivals become asymptotic (Fig. 2). As a result, a linear move-out (LMO) was applied to mute out the refracted arrivals. As no arrivals moved, it is assumed that

there are no refracted arrivals coincident with reflected arrivals. Multiple suppression techniques were attempted using a Tau-P transform and an F-K filter, but neither approach improved the imaging. Dip move-out (DMO) was applied to remove coherent noise, but this caused additional aliasing within the data. In addition, Kirchhoff migration was applied, but this met with minimal results due to the lack of near-source information and near surface velocity control (Table 1). These attempted methods failed to improve result quality and therefore were not used for the final reflection stack.

Table 1:
Generalized Processing Steps for Silver Hills Seismic Reflection Profile

Data Reformat	SEGY → ProMAX®
Geometry	Assign station and shot coordinates
Muting	Top mute
Trace edit	Remove noisy traces
AGC	500 msec root mean square gain window to adjust amplitudes
Static Shift	Elevation Static shift to sea-level
Deconvolution	192 ms length, 160 ms predictor, 0.1% white noise, Multiple removal
Interval Velocity Model	Model developed from literature (Boynton et al., 1979, Christeson et al., 2008)
NMO	30% stretch mute, Multiple removal
Bandpass Filter (Hz)	2-4-30-45 Hz Butterworth
Stack	Zero-offset mean Stack

Tested processes not used

LMO	Linear move-out in time domain, reduced velocity 6000 m/s, attempt to remove refractions
DMO	Dip move-out in time domain, attempt to remove coherent noise
Semblance	Velocity Analysis
Tau-P	Parabolic Radon Transform, attempt to remove multiples
F-K filter	Filter in frequency and wavenumber, attempt to remove multiples
Migration	Kirchhoff Time Migration, attempt to enhance image and place reflectors in correct place

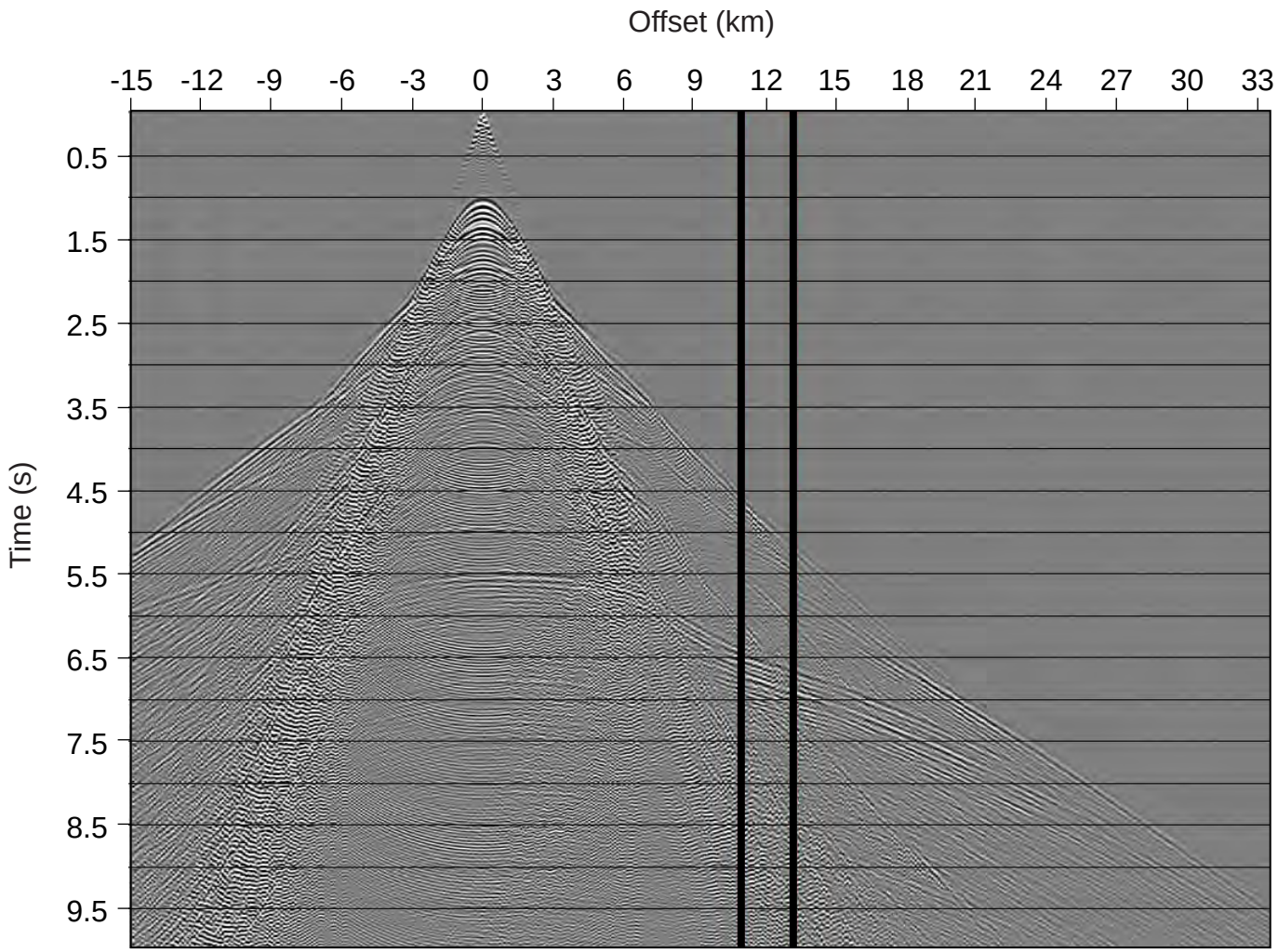

Figure 2: Synthetic seismic shot gather showing typical move-out if the receivers were continuous from the source. Black bars show the location of the Silver Hills seismic reflection gathers. As a result of these large offsets, typical reflection hyperbolas are not easily distinguished from linear refractions and the lack of near-source data proved to be a challenge in the processing.

CHAPTER 5 RESULTS

Processing of the SHP produced an image of the crustal structure east of Montserrat on three profiles (Fig. 1). Located ~7 km to the east of Silver Hills and covering a length of ~4.5 km from north to south, the Silver Hills 560 reflection profile has produced the best quality image (Fig. 3). Two reflections were identified, one at 5 s (~12 km) and one at 9 s (~23 km) (Fig. 3). Both reflectors have positive reflection coefficients, which indicate an increase in velocity and density across these interfaces. Multiples still remain within the data and are clearly visible below Reflector 2 (Fig. 3). The other two parallel lines, 540 and 550 showed a weaker Reflector 1 (2.5 s twt and 4.0 s twt respectively), and no Reflector 2 was visible (Appendix E, Fig. 19 and 20).

The Lesser Antilles crust, located within the Caribbean, ranges from 22 to over 30 km in thickness (Boynton et al., 1979; Wadge, 1994; Christeson et al., 2008). Our data shows a crustal thickness east of Montserrat of ~23 km (Fig. 3c), which is consistent with some previous studies (e.g., Case et al., 1984; Christeson et al., 2008), but is less than the estimate of Sevilla et al. (manuscript in review, 2009) for southern and western Montserrat. Sevilla et al. (manuscript in review, 2009) has used a crustal model with an average velocity of 6.18 km/s to estimate crustal thickness using receiver functions. Our study uses a velocity model with an average crustal velocity of 6.14 km/s developed from

existing refraction data. Both these velocity models are consistent, so therefore the discrepancy may suggest that the Moho dips significantly around Montserrat.

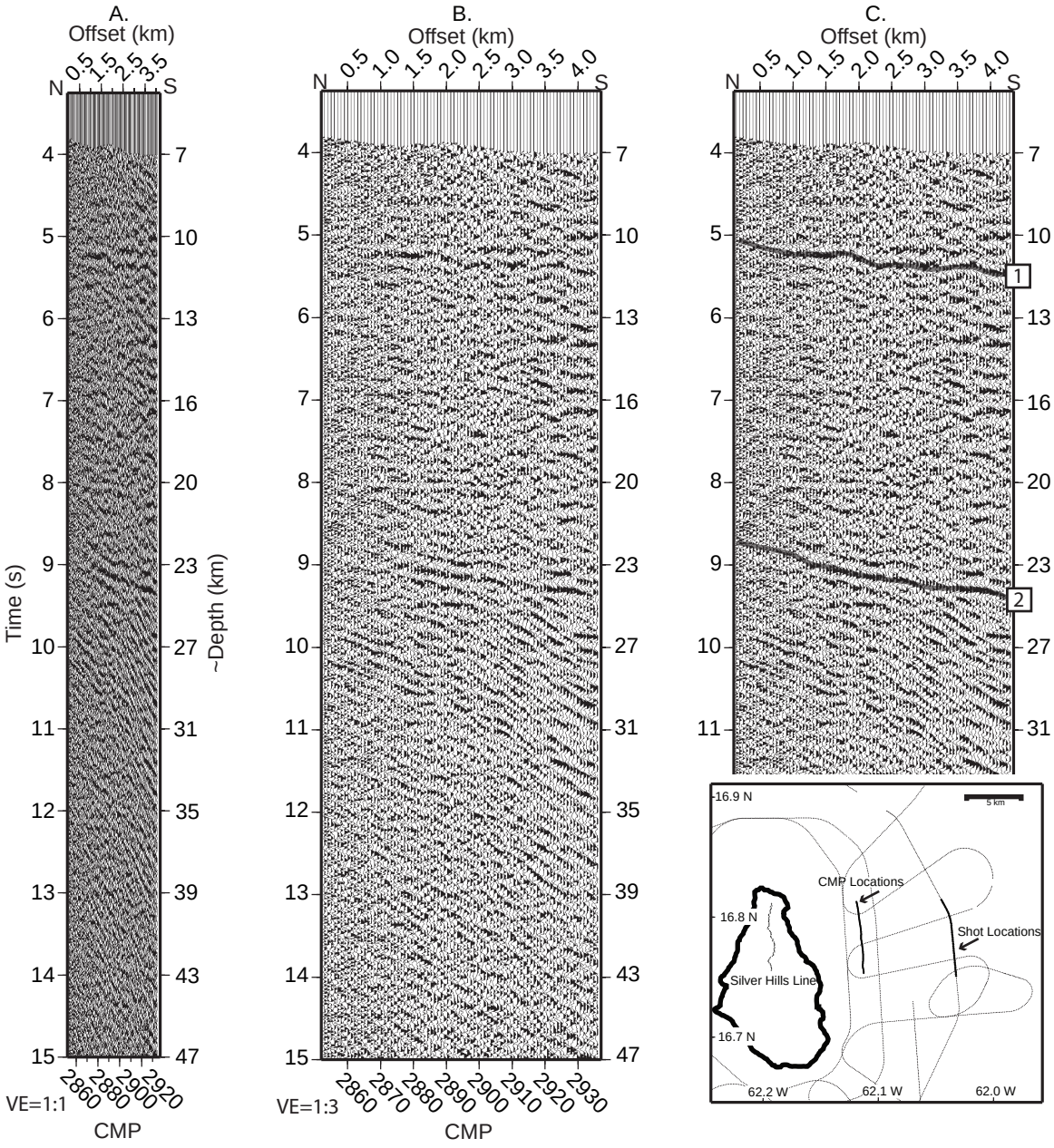

Figure 3: The processed Silver Hills 560 reflection stack that is approximately 6 km offshore Montserrat (see inset) is displayed in 3 panels (a, b, c). (a) Displayed data with no vertical exaggeration has two reflections appearing at ~5 s (depth ~12 km, dip ~15°) and at 9 s (depth ~23 km, dip ~25°). (b) Horizontal exaggeration 1:3 (c) Interpreted section with Reflector 1 at 5 s and Reflector 2 at 9 s. Both reflections have a stronger reflectivity than others within the stacked section.

CHAPTER 6 INTERPRETATION

The cause of reflections within the crust are non-unique and are effected by composition, density, porosity, fluid content and temperature (e.g., Holbrook et al., 1999). We considered four alternative "working hypotheses" to interpret the mid-crustal reflector (Reflector 1, Fig. 3): a) changes in crustal rock composition: b) change in coherence, from fractured rock to virtually non-fractured rock: c). A lithologic change from sediments to oceanic crust: and d) a magmatic sill embedded within the crust (Fig. 4).

The reflection coefficient was calculated for Reflector 1 in order to compare with our models using the average velocity above the reflector (layer 1, velocity 4.94 km/s) and below the reflector (layer 2, velocity 6.68 km/s). Gardner's equation (Gardner et al., 1974) was used to estimate the average density (layer 1, 2.60 kg/m^3 and layer 2, 2.80 kg/m^3) of the rock making up these two layers. These values give a reflection coefficient of 0.18 (Table 2).

Working in reverse order, a magma sill within the oceanic lithosphere would be expected to have a negative impedance (Brown et al., 1979). Reflector 1 has a positive impedance contrast, so this model can be rejected. With respect to sediments over oceanic crust, an acoustic basement beneath 12 km of sediments was reported in the Grenada Basin (Holcombe et al., 1990). However, it is not conceivable that 12 km of sediments could exist near the volcanic arc axis only 7 km off the coast of an active

volcanic island (Boynton et al., 1979; Christeson et al., 2008, Fig. 13). In addition, the calculated reflection coefficient of 0.38 is too large for Reflector 1 (Table 2). A sharp transition from fractured to non-fractured rock (Holbrook et al., 1999) gives a reflection coefficient of 0.16, 0.20, and 0.20, for fractured basalt, fractured andesite and fractured granite to respectively (Table 2) and have a standard deviation of 0.02. The fractured materials over mafic material are consistent with Reflector 1 (Fig. 3). As a result, our data is consistent with changes in crustal rock composition, and a change in coherence, from fractured rock virtually non-fractured rock.

Within the Lesser Antilles, under a surficial low velocity layer, two crustal layers have been reported-- an upper layer with velocities of ~6.1-6.3 km/s, and a lower layer with velocities of ~6.9-7.3 km/s (Boynton et al., 1979; Christeson et al., 2008). These two layers are consistent with a intermediate-felsic rock over mafic material (Boynton et al., 1979; Christensen and Mooney, 1995). In addition, a felsic (tonolite) mid-crustal layer has been interpreted from other island arcs such as the Solomon islands, Izu-Bonin, Tonga, and the South Sandwich islands (Taira et al., 1998; Kodaira et al., 2007; Leat et al., 2007; Saito et al., 2007). Geochemical analysis of xenoliths taken from deposits on Montserrat reveal a variable chemical composition of SiO_2 up to 77.7% (Rea, 1974). The formation of such high silica value within metamorphic xenoliths suggest a concentration of felsic material may exist within the crust (Rea, 1974).

Reflection coefficients for both granite (velocity 6.23 km/s, density 2.66 kg/m^3) and andesite (velocity 5.54 km/s, density 2.63 kg/m^3) (Christensen and Mooney, 1995) gave impedance values 0.01, and 0.08 respectively (Table 2). However, if the material is a fractured felsic-intermediate material, then we can calculate reflection coefficients of

0.20. This preferred model of fractured felsic mid-crust above a mafic lower crust supports the proposition that a mid-crust felsic layer maybe common in oceanic island arcs (Taira et al., 1998).

Table 2: Velocity, density and calculated reflection coefficient values. (A). Velocity and density data from Christensen and Mooney (1995), at 10 km depth. (B) Velocity calculated from interval velocity model; density calclulated using Gardner's equation (Gardner et al., 1974). (C) Calculated reflection coefficients for this study and potential models.

(A) Rock Type	Vel. (km/s)	Density (kg/m^3)	Impedance (km kg/ s m^3)
Basalt	5.89	2.88	16.99
Andesite	5.54	2.63	14.56
Granite	6.23	2.66	16.57
Sandstone	3.30	2.30	7.59
Fractured Basalt	4.30	2.88	12.40
Fractured Andesite	4.30	2.63	11.31
Fractured Granite	4.30	2.66	11.44

(B) This Study	Avg. Vel. (km/s)	Avg. Density (kg/m^3)	Impedance (km kg/ s m^3)
Layer 1	4.96	2.60	12.90
Layer 2	6.68	2.80	18.70
Reflection Coefficient	0.18		

(C) Potential Models	Reflection Coefficient
Andesite/Basalt	0.08
Granite/Basalt	0.01
Sandstone/Basalt	0.38
Fractured Basalt/Basalt	0.16
Fractured Andesite/Basalt	0.20
Fractured Granite/Basalt	0.20
This Study	0.18

Figure 4: Four proposed models to account for Reflector 1(Figure 3c). Reflector 1 may be explained by: (a) changes in crustal composition from intermediate to mafic; (b) cohesive change from fractured to non-fractured material; (c) lithologic change from sediments to oceanic crust; (d) a mag matic sill within the oceanic lithosphere.

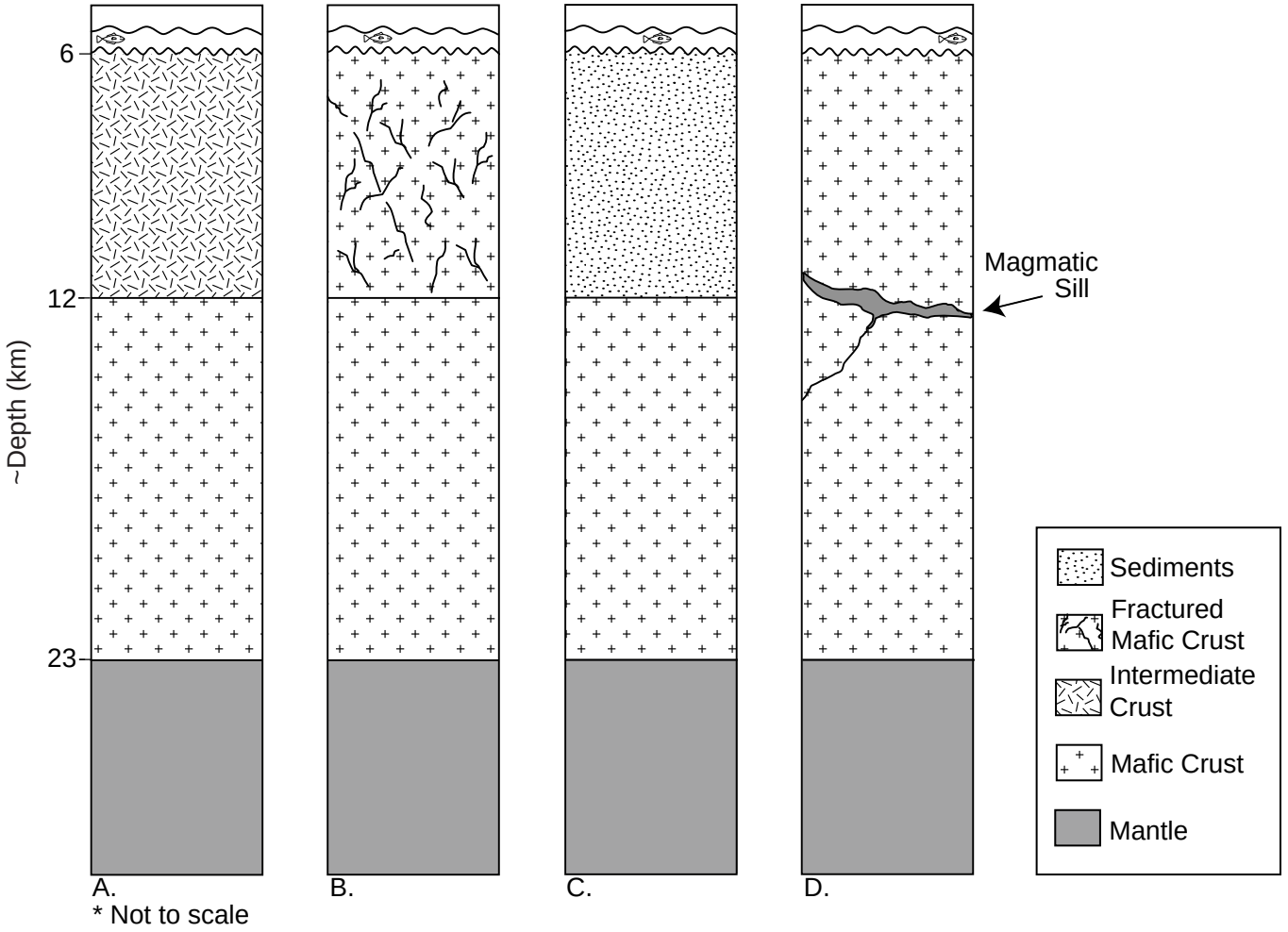

CHAPTER 7 CONCLUSION

Knowledge of the structure and composition of island arc crust is key to understanding the generation and evolution of continental crust [Christensen and Mooney, 1995; Keller et al., 2005; Takahashi et al., 2007; Sevilla et al., manuscript in review, 2009]. The crustal structure off the coast of Montserrat is consistent with previous studies within island arcs that reveal (under a surficial layer of sediments and lavas), two crustal layers -- an upper layer of intermediate material with velocities of ~6.0-6.3 km/s, and a lower mafic crust with a velocity about 6.9 or 7.0 km/s [Boynton, et al., 1979; Taira, et al., 1998; Kodaira, et al., 2007; Leat, et al., 2007; Saito, et al., 2007; Paulatto, et al., in press, Sevilla, et al., in review, 2009]. Our analysis and interpretation of the SHP 540, 550 and 560 suggests that the contact between the upper and lower crustal layers is located at ~4 km (twt 3 s profile 540), 6 km (twt 4 s profile 550), and 12 km (twt 5 s profile 560) depths within the crust, moving west from the island, and has a similar structure to that found in the lower Lesser Antilles (Officer et al., 1957; Boynton et al., 1979). In particular, the LASP seismic refraction study revealed the upper/lower layer boundary occurs at variable depths, deeper between some island clusters, but is at 10-12 km depth under Guadeloupe and Dominica (the two islands nearest to Montserrat on the south) (Boynton et al., 1979, Fig. 6). This depth is very consistent with our result.

Our reflection data suggest that the Moho depth off northeast Montserrat is ~23 km. This result is consistent with Moho depth contours presented by Case et al. (1984)

(Fig. 5). However Moho depths of 28-32 km were suggested by receiver function data [Sevilla et al., manuscript in review, 2009] for regions west and south of Montserrat. The difference in results suggests local variability, and indeed our result indicates for the Moho reflector a substantial apparent southward dip of 25^{o} (Fig. 3c). A possible increase of Moho depth of $\geq$4 km is implied by extrapolating the reflector a distance of 9 km, to the south coast of Montserrat. The implication is that our result and those of Sevilla et al. (in review, 2009) are not inconsistent. The Aleutian island arc has a reported depth of 25-30 km (Holbrook et al., 1999) and the Izu-Bonin arc has a depth of 26-32 km (Kodaira et al., 2007), suggesting that the crustal thicknesses reported for Montserrat are comparable.

Finally, crustal thickening and modification would be needed to convert this island arc into typical continental crust. The crustal composition proposed by our model suggests that the island arc near Montserrat is undergoing compositional changes toward a more felsic material, as indeed also suggested by the volcanic products observed. This also suggests that the mid-crust felsic material found in other island arcs such as the Sandwich, Izu-Bonin, and Solomon islands maybe more common than originally thought (Taira et al., 1998; Kodaira et al., 2007; Leat et al., 2007; Saito et al., 2007). This may be an early step in the evolution toward arc crust maturity.

Figure 5: Map of the Lesser Antilles showing the estimated depth to the Moho (triangles) [after Case, et al., 1984] with added Montserrat data from the SEA-CALIPSO experiment (circle), contour interval spacing at 2 km. Montserrat, shown with black box, has a crustal thickness of ~23 km approximately 6 km off its east coast. Current active volcanic islands, called the Volca nic Caribbees include: Saba, St. Eustatius, St. Kitts, Nevis, Redonda, Montserrat, Guadeloupe and Dominica, Martinique, St. Lucia, St. Vincent and Grenada. The Limestone Caribbees; Anguilla, Barbuda and Antiqua are of an extinct Eocene to mid-Oligocene volcanic chain [e.g., Pindell, 1994].

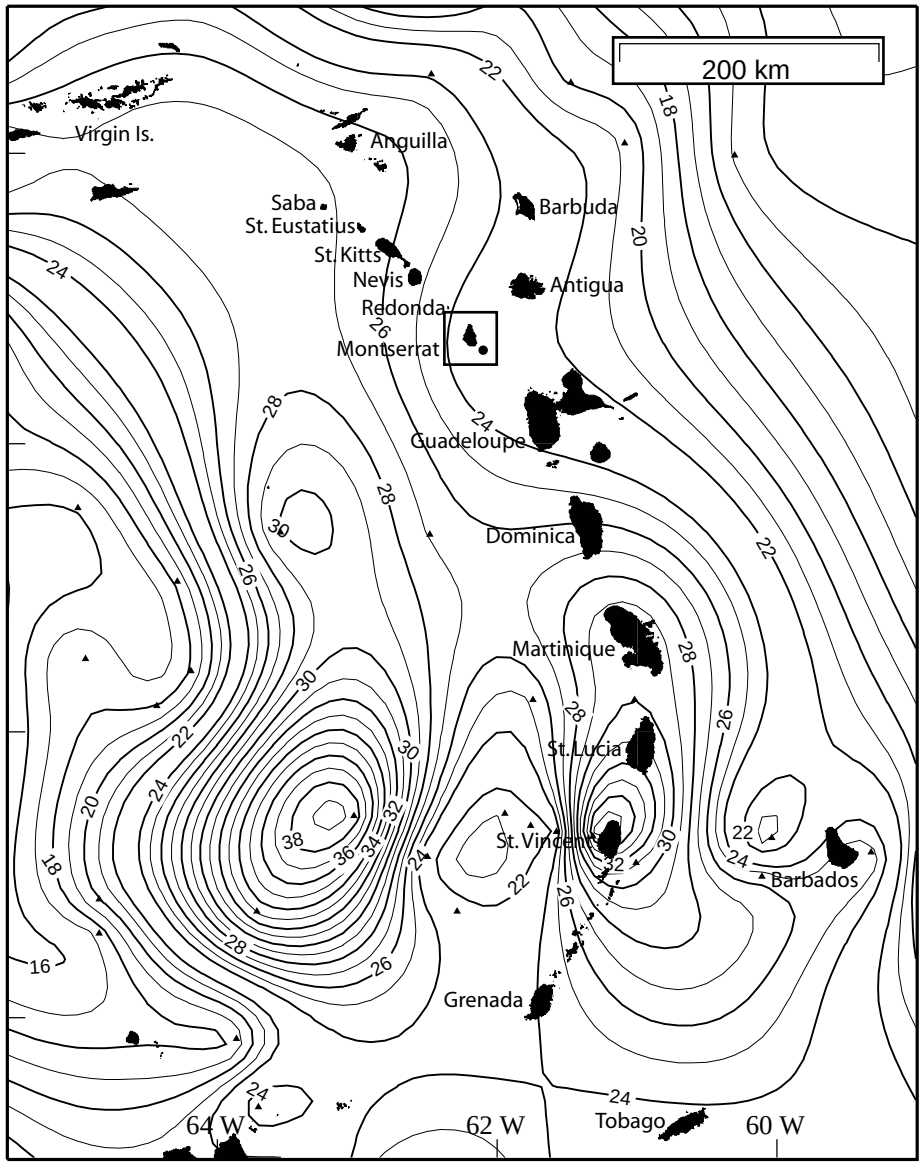

REFERENCES

Aspinall, W. P., Miller, A. D., Lynch, L. L., Latchman, J. L., Stewart, R. C., White, R. A., and Power, J. A., 1998, Soufriere Hills Eruption, Montserrat, 1995-1997: Volcanic Earthquake Locations and Fault Plane Solutions: Geophysical Research Letters, v. 25, no. 18, p. 3397-3400.

Baker, P. E., 1984, Geochemical Evolution of St Kitts and Montserrat, Lesser Antilles: J. geol. Soc. London, v. 141, p. 401-411.

Baptie, B., Luckett, R., and Neuberg, J., 2002, Observations of Low-Frequency Earthquakes and Volcanic Tremor at Soufriere Hills Volcano, Montserrat, *in* Druitt, T. H., and Kokelaar, B. P., eds., The Eruption of Soufriere Hills Volcano, Montserrat, from 1995 to 1999: London, Geological Society of London, p. 611-620.

Bouysse, P. and Guennoc, P., 1983, Data on the Structure of the Insular Arc in the Lesser-Antilles, between St-Lucia and Anguilla: Marine Geology, v. 53, no. 1-2, p. 131-166.

Bouysse, P. and Westercamp, D., 1990, Subduction of Atlantic Aseismic Ridges and Late Cenozoic Evolution of the Lesser Antilles Island-Arc: Tectonophysics, v. 175, no. 4, p. 249.

Boynton, C. H., Westbrook, G. K., Bott, M. H. P., and Long, R. E., 1979, A Seismic Refraction Investigation of Crustal Structure beneath the Lesser Antilles Island Arc: Geophysical Journal International, v. 58, p. 371-393.

Brown, L. D., Krumhansl, P. A., Chapin, C. E., Sanford, A. R., Cook, F. A., Kaufman, S., Oliver, J. E., and Schilt, F. S., 1979, Cocorp Seismic Reflection Studies of the Rio Grande Rift, *in* Riecker, R. E., ed., Rio Grande Rift: Tectonics and Magmatism: Washington, D. C., American Geophysical Union.

Case, J. E., Holcombe, T. L., and Martin, R. G., 1984, Map of the Geologic Provinces in the Caribbean Region, *in* Bonini, W. E., Hargraves, R. B., and Shagam, R., eds., The Caribbean-South American Plate Boundary and Regional Tectonics, Geological Society of America Memoir 162, p. 1-30.

Christensen, N. I. and Mooney, W. D., 1995, Seismic Velocity Structure and Composition of the Continental Crust: A Global View: Journal of Geophysical Research, v. 100, no. B7, p. 9761-9788.

Christeson, G. L., Mann, P., Escalona, A., and Aitken, T. J., 2008, Crustal Structure of the Caribbean-Northeastern South America Arc-Continent Collision Zone: Journal of Geophysical Research, v. 113.

Donnelly, T. W., 1994, The Caribbean Sea Floor, Caribbean Geology: An Introduction: Kingston, UWI Publishers' Association.

Draper, G., Jackson, T. A., and Donovan, S. K., 1994, Geologic Provinces of the Caribbean Region, Caribbean Geology: An Introduction: Kingston, UWI Publishers' Association.

Druitt, T. H. and Kokelaar, B. P., 2002, The Eruption of Soufriere Hills Volcano, Montserrat, from 1995 to 1999, Geological Society Memoirs No. 21: London, Memoirs No. 21, Geological Society.

Druitt, T. H., Young, S. R., Baptie, B., Bonadonna, C., Calder, E. S., Clarke, A. B., Cole, P. D., Harford, C. L., Herd, R. A., Luckett, R., Ryan, G., and Voight, B., 2002, Episodes of Cyclic Vulcanian Explosive Activity with Fountain Collapse at Soufriere Hills Volcano, Montserrat, *in* Druitt, T. H., and Kokelaar, B. P., eds., The Eruption of Soufriere Hills Volcano, Montserrat, from 1995 to 1999: London, Geological Society of London, p. 281-306.

Feuillet, N., Manighetti, I., Tapponnier, P., and Jacques, E., 2002, Arc Parallel Extension and Localization of Volcanic Complexes in Guadeloupe, Lesser Antilles: Jornal of Geophysical Research - Solid Earth, v. 107, no. B12.

Francis, P. and Oppenheimer, C., 2004, Types of Volcanic Activity, Volcanoes: New York, Oxford University Press, p. 107-135.

Gardner, G. H. F., Gardner, L. W., and Gregory, A. R., 1974, Formation Velocity and Density -- the Diagnostic Basics for Stratigraphic Traps: Geophysics, v. 39, p. 770-780.

Herd, R. A., Edmonds, M., and Bass, V. A., 2005, Catastrophic Lava Dome Failure at Soufriere Hills Volcano, Montserrat, 12-13 July 2003: Journal of Volcanology and Geothermal Research, v. 148, p. 234-252.

Holbrook, W. S., Lizarralde, D., McGeary, S., Bangs, N., and Diebold, J., 1999, Structure and Composition of the Aleutian Island Arc and Implications for Continental Crustal Growth: Geology, v. 27, no. 1, p. 31-34.

Holcombe, T. L., Ladd, J. W., Westbrook, G., Edgar, N. T., and Bowland, C. L., 1990, Caribbean Marine Geology; Ridges and Basins of the Plate Interior, *in* Dengo, G., and Case, J., eds., The Caribbean Region: Boulder, Colorado, Geological Society of America, p. 231-260.

Kodaira, S., Sato, T., Takahashi, N., Ito, A., Tamura, Y., Tatsumi, Y., and Kaneda, Y., 2007, Seismological Evidence for Variable Growth of Crust Along the Izu Intraoceanic Arc: Journal of Geophysical Research, v. 12.

Kokelaar, B. P., 2002, Setting, Chronology and Consequences of the Eruption of Soufriere Hills Volcano, Montserrat (1995-1999), *in* Druitt, T. H., and Kokelaar, B. P., eds., The Eruption of Soufriere Hills Volcano, Montserrat, from 1995 to 1999: London, Geological Society of London, p. 1-43.

Leat, P. T., Larter, R. D., and Millar, I. L., 2007, Silicic Magmas of Protector Shoal, South Sandwich Arc: Indicators of Generation of Primitive Continental Crust in an Island Arc: Geol. Mag., v. 144, no. 1, p. 179-190.

Macdonald, R., Hawkesworth, C. J., and Heath, E., 2000, The Lesser Antilles Volcanic Chain: A Study in Arc Magmatism: Earth-Science Reviews, v. 49, p. 1-76.

MacGregor, A. G., 1938, The Royal Society Exedition to Montserrat, B.W.I. The Volcanic History and Petrology of Montserrat, with Observations on Mt Pele, in Martinique: Philosophical transactions of the Royal Society of London Series B, Biological Sciences, v. 229, no. 557, p. 1-90.

Magnani, M. B., Zelt, C. A., Levander, A., and Schmitz, M., 2009, Crustal Structure of the South American-Caribbean Plate Boundary at 67w from Controlled Source Seismic Data: J. Geophys. Res., v. 114, no. B02312.

Neuberg, J., Baptie, B., Luckett, R., and Stewart, R., 1998, Results from the Broadband Seismic Network on Montserrat: Geophysical Research Letters, v. 25, no. 19, p. 3661-3664.

Officer, C. B., Ewing, J. I., Edwards, R. S., and Johnson, H. R., 1957, Geophysical Investigations in the Eastern Caribbean: Venezuelan Basin, Antilles Island Arc, and Puerto Rico Trench: Bulletin of the Geological Society of America, v. 68, no. March, p. 359-378.

Pindell, J. L., 1994, Evolution of the Gulf of Mexico and the Caribbean, Caribbean Geology: An Introduction: Kingston, UWI Publishers' Association.

Power, J. A., Wyss, M., and Latchman, J. L., 1998, Spatial Variations in the Frequency-Magnitude Distribution of Earthquakes at Soufriere Hills Volcano, Montserrat, West Indies: Geophysical Research Letters, v. 25, no. 19, p. 3653-3656.

Rea, W. J., 1974, The Volcanic Geology and Petrology of Montserrat, West Indies: Journal of the Geological Society, v. 130, p. 341-366.

Saito, S., Arima, M., Nakajima, T., Misawa, K., and Kimura, J.-I., 2007, Formation of Distinct Granitic Magma Batches by Partial Melting of Hybrid Lower Crust in the Izu Arc Collision Zone, Central Japan: Journal of Petrology, v. 48, no. 9, p. 1761-1791.

Smith, A. L., Roobol, M. J., Schellekens, J. H., and Mattioli, G. S., 2007, Prehistoric Stratigraphy of the Soufriere Hills - South Soufriere Hills Volcanic Complex, Montserrat, West Indies: The Journal of Geology, v. 115, p. 115-127.

Taira, A., Saito, S., Aoike, K., Morita, S., Tokuyama, H., Suyehiro, K., Takahashi, N., Shinohara, M., Kiyokawa, S., Naka, J., and Klaus, A., 1998, Nature and Growth

Rate of the Northern Izu-Bonin (Ogasawara) Arc Crust and Their Implications for Continental Crust Formation: The Island Arc, v. 7, p. 395-407.

Voight, B., Linde, A., Sacks, I. S., Mattioli, G. S., Sparks, R. S. J., Elsworth, D., Hidayat, D., Malin, P. E., Shalev, E., Widiwijayanti, C., Young, S. R., Bass, V., Clarke, A. B., Dunkley, P., Johnston, W., McWhorter, N., Neuberg, J., and Williams, P., 2006, Unprecedented Pressure Increase in Deep Magma Reservoir Triggered by Lava-Dome Collapse: Geophysical Research Letters, v. 33, p. L03312.

Wadge, G., 1994, The Lesser Antilles, Caribbean Geology: An Introduction: Kingston, UWI Publishers' Association.

Wessel, P. and Smith, W. H. F., 2006, Generic Mapping Tool (Gmt): Manoa, Hawaii.

White, R. A., Miller, A. D., Lynch, L., and Power, J., 1998, Observations of Hybrid Seismic Events at Soufriere Hills Volcano, Montserrat: July 1995 to September 1996: Geophysical Research Letters, v. 25, no. 19, p. 3657-3660.

Yilmaz, O., 2001, Seismic Data Analysis: Processing, Inversion, and Interpretation of Seismic Data, Investigations in Geophysics No. 10: Tulsa, Society of Exploration Geophysics, 2027 p.

APPENDIX A: EXPANDED TECTONIC BACKGROUND

GEOLOGIC BACKGROUND

During the late Jurassic through the Early Cretaceous (112-99.6 Ma), as a consequence of seafloor spreading, the Proto-Caribbean plate formed, and North and South America separated (e.g., Draper et al., 1994; Pindell, 1994). As the Proto-Caribbean formed, the Farallon plate was actively subducting beneath the Proto-Caribbean (e.g., Pindell, 1994). During the Early Cretaceous (125-112 Ma), subduction reversed, and the Proto-Caribbean plate began subducting beneath the Farallon plate (Fig. 6) (e.g., Draper et al., 1994; Pindell, 1994). The reverse of the subduction direction was either due to the arrival of the buoyant, thick, oceanic plateau located on the Farallon plate, or the plateau was extruded as a result of the back thrust, caused by the reverse in subduction direction (e.g., Draper et al., 1994; Pindell, 1994). By the Late Cretaceous (85.8-83.5 Ma), onset of a new subduction zone on the western edge of the buoyant oceanic plateau created the Panama Costa Rica Arc, isolating the Caribbean as its own plate (Fig. 6) (e.g., Draper et al., 1994; Pindell, 1994).

The structure of the Lesser Antilles consists of the Atlantic oceanic crust; the forearc; the Lesser Antilles; and the Grenada Basin, which lies behind the arc (Fig. 7) (e.g., Wadge, 1994). The island arc consists of, (from north to south): the Volcanic Caribbees; Saba, St. Eustatius, St. Kitts, Redonda, Montserrat; Guadeloupe and Dominica; merging with the western Limestone Caribbees, which consist of Barbuda, Antiqua and a few smaller islands, at Martinique where the two arcs merge into one and

continue south with St. Lucia, St. Vincent and Grenada (Fig. 8) (e.g., Baker, 1984). From Martinique northwards, the extinct eastern volcanic chain of the Lesser Antilles, characterized by Cenozoic limestones, are dated by their volcanics as Eocene to mid-Oligocene in age (55.8-28.4 Ma) (e.g., Pindell, 1994). The north-western active chain, extending north from Montserrat to Saba, consists of smaller islands whose volcanoes are smaller than the central Lesser Antilles islands (Fig. 8) (Wadge, 1994; Kokelaar, 2002). These islands lie on oceanic crust that is no more than 30 km thick above an athenospheric wedge that extends from 130 km to 210 km down (Kokelaar, 2002).

The island of Montserrat formed in the Miocene when the axis of the northern arc migrated westwards (~23 Ma) (Baker, 1984; Kokelaar, 2002). The island is made up of four volcanic complexes, Silver Hills (SH), Centre Hills (CH), Soufriere Hills (SHV) and South Soufriere Hills (SSH), which are of Pleistocene age (1.6 Ma) (e.g., Baker, 1984; Herd et al., 2005). The SHV is an andesite dome-building volcano located on south Montserrat (Druitt et al., 2002; Herd et al., 2005). The 400 ka history of SHV and SSH shows periods of irregular activity spanning thousands of years punctuated by long periods of dormancy (e.g., Smith et al., 2007). Stratigraphy of the SH-SSH complex shows that Pelean-style activity dominates their history (e.g., Smith et al., 2007). The current explosive behavior of Montserrat, however, is classified as vulcanian behavior, characterized by brief violent explosions and eruption columns rising 10-20 km (Francis and Oppenheimer, 2004; Smith et al., 2007). This behavior is attributed to the interaction of magma with external water, emptying the conduit to a depth of 0.5 to 2 km or more (Druitt et al., 2002).

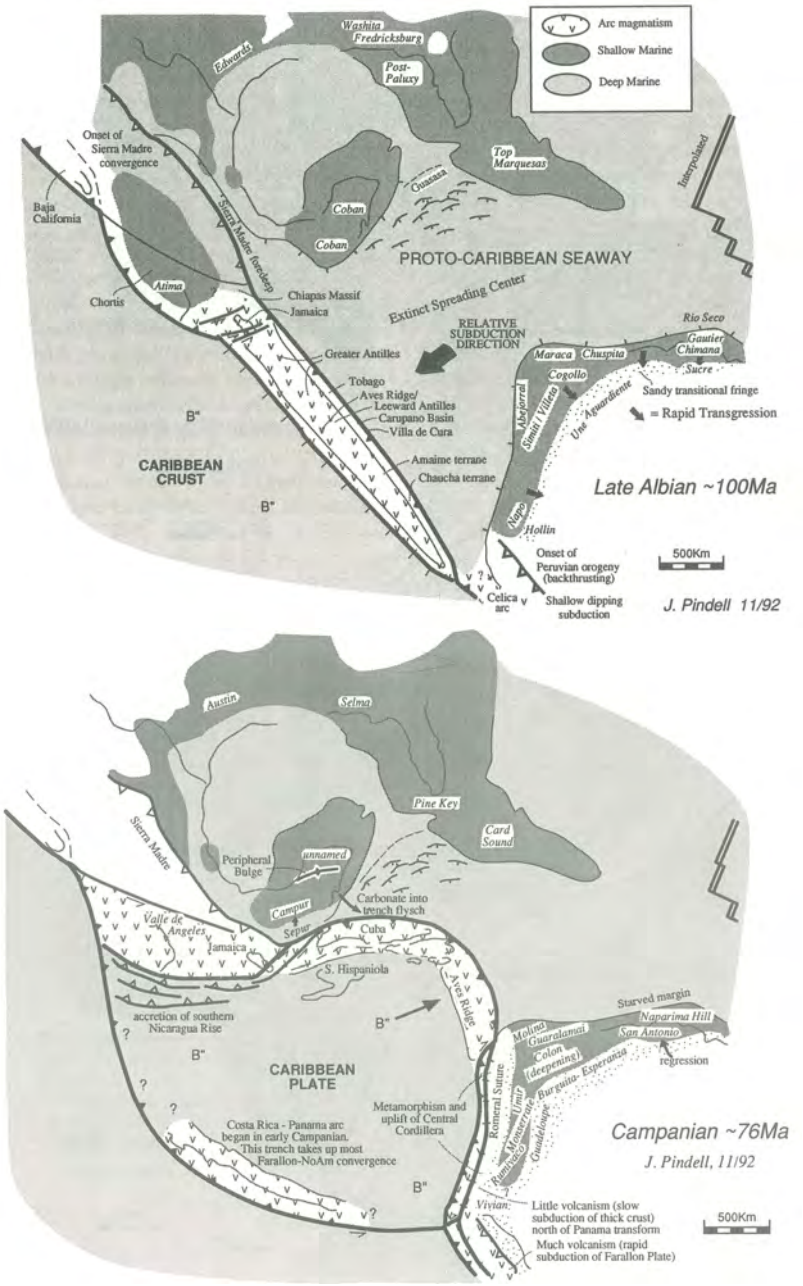

Figure 6: Top. Subduction of the Farallon plate was occuring beneath the eastern Proto-Caribbean plate during the Early Cretaceous, at this time however, subduction flipped polarity from the Farallon Plate to the subduction of the Proto-Caribbean plate due to the arrival of the bouyant oceanic plateau (marked B") (from Pindell, 1994). Bottom. Onset of new subduction creates the Panama-Coasta Rica Arc and isolates the Caribbean as its own plate for the first time (from Pindell, 1994)

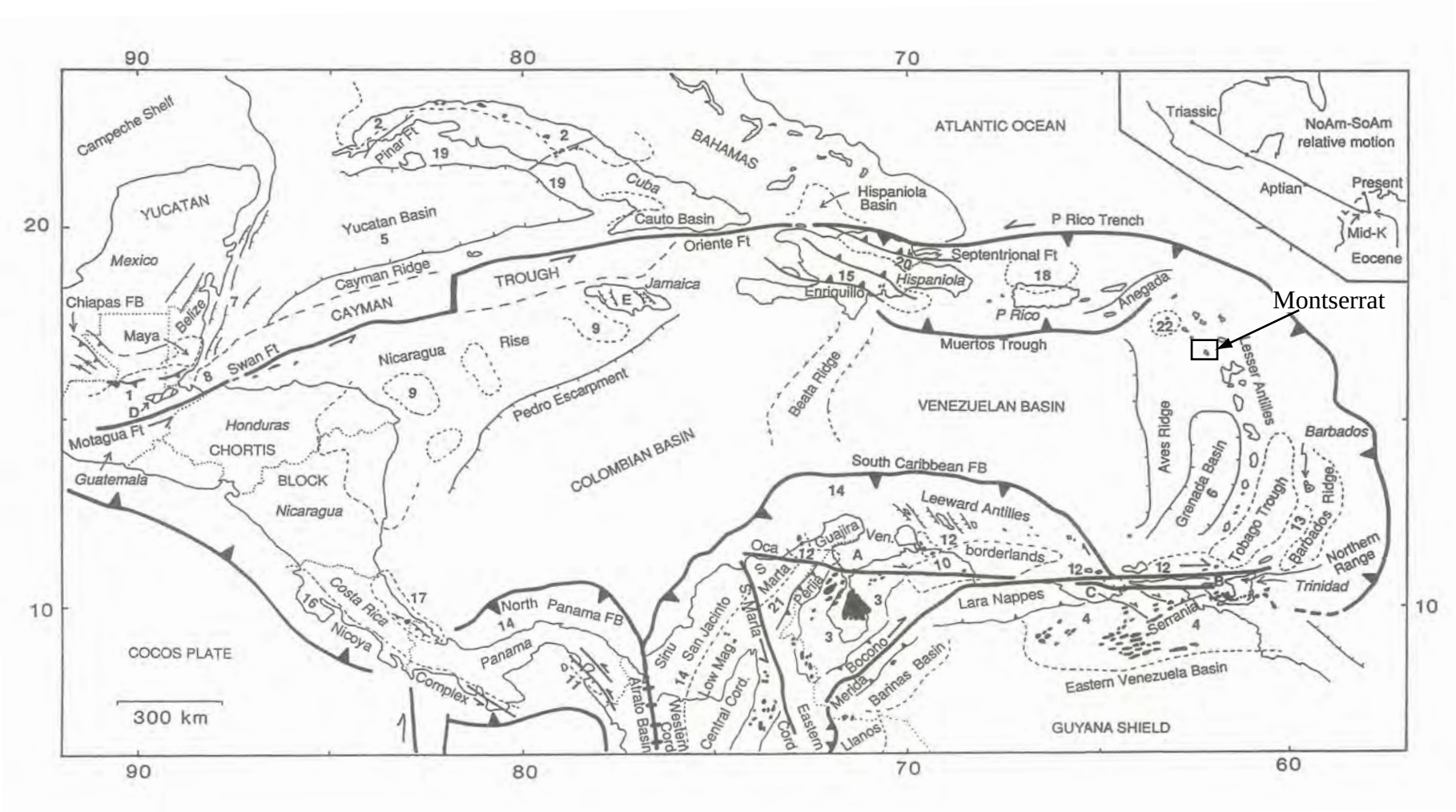

Figure 7: Tectonic structure of the Caribbean plate (from Pindell, 1994). The island of Montserrat (black box) is located on the northern portion of the Lesser Antilles and is one of several islands created by the island arc on the western edge of the Caribbean plate. Listed numbers correspond to basins discussed in Pindell's Evolution of the Gulf of Mexico and the Caribbean (Pindell, 1994).

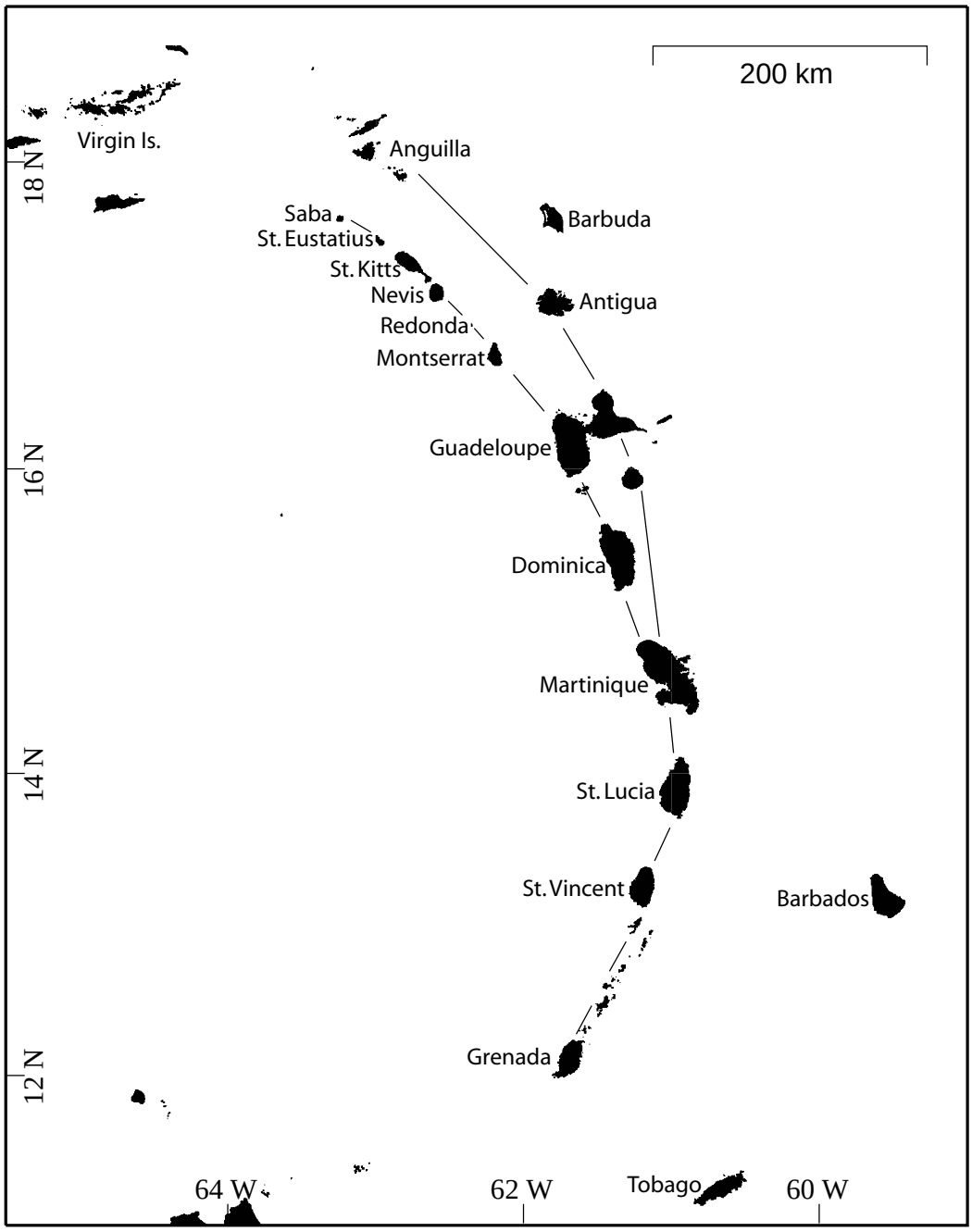

Figure 8: Map of the Lesser Antilles. The lines connecting the islands show the inner active island arc and the outer extinct (Limestone Caribbees) arc. The Lesser Antilles consists of, (from north to south): The Volcanic Caribbees; Saba, St. Eustatius, St. Kitts, Nevis, Redonda, Montserrat, Guadeloupe and Dominica; merging with the western Limestone Caribbees, Anguilla, Barbuda, and Antiqua, and continuing south, Martinique, St. Lucia, St. Vincent and Grenada.

APPENDIX B: EXPANDED GEOPHYSICAL BACKGROUND

PREVIOUS GEOPHYSICAL STUDIES OF THE CARIBBEAN

GRAVITY

Gravity surveys in the Caribbean reveal positive anomalies over the arc massif and negative anomalies over the forearc of the Caribbean plate (e.g., Wadge, 1994). The positive gravity anomaly is due to the relatively high crustal level of dense igneous rock composing the islands (e.g., Wadge, 1994). In contrast, the negative anomalies, are due to the sedimentary rocks composing the accretionary wedge (e.g., Wadge, 1994).

SEISMIC REFLECTION/REFRACTION DATA

Seismic refraction/reflection data indicate that the oceanic crust of the Caribbean is unusually thick, upwards of 30 km, due to the oceanic plateau extruded above the oceanic plate (e.g., Donnelly, 1994). Three crustal layers, an upper sedimentary layer and two lower crustal layers, were identified in the Lesser Antilles Seismic Project (LASP 1972) (Boynton et al., 1979; Wadge, 1994). The LASP experiment was conducted just south of Montserrat starting at Guadeloupe and extending south to Grenada (Boynton et al., 1979). This study determined that the upper 10-30 km has velocities of 6.3 km/s and 7.0 km/s and greater for the upper mantle (Boynton et al., 1979). Although the resolution of the LASP data did not allow for the velocity definition of the sedimentary layers, another seismic refraction experiment indicated an average

velocity of 3.3 km/s (e.g., Officer et al., 1957; Boynton et al., 1979). This layer is comprised of sediments, lavas and pyroclastic material and has two distinct reflectors appearing uniformly throughout the Caribbean basins (Boynton et al., 1979; Wadge, 1994). The second layer, with an average velocity of 6.2-6.3 km/s, is indicative of compositions similar to intermediate plutonic rocks (Boynton et al., 1979; Wadge, 1994). The lower layer has an average velocity of 6.9-7.0 km/s which is dominated by basic rocks and likely made up of gabbros and basic cumulates left in magma chambers (Boynton et al., 1979; Wadge, 1994).

GEODETIC MEASUREMENTS

The Caribbean Andesite Lava Island Precision Seismo-geodetic Observatory (CALIPSO) experiment investigated the Soufriere Hills Volcano in an attempt to better understand its magmatic system (Voight et al., 2006). The experiment included an integrated array of instruments in four boreholes 100 m deep that recorded the July 2003 dome collapse, allowing a wealth of data to be acquired (Voight et al., 2006). Geodetic modeling of the radial strain recorded reveals that the magma chamber is likely an oblong ellipsoid at a depth of 5-6 km (Voight et al., 2006).

VOLCANO-TECTONIC SEISMIC STUDIES

Seismic studies reveal that long period and volcano tectonic earthquakes on Montserrat are associated with magmatic processes below the SHV (Power et al., 1998; White et al., 1998; Baptie et al., 2002). The hypocenter for these earthquakes are greater than 2-3 km depth (Neuberg et al., 1998; White et al., 1998). Spatial distribution of the

hypocenters for the earthquakes suggest a minimum depth of 5 km for the magma body (Aspinall et al., 1998).

APPENDIX C: GEOMETRY

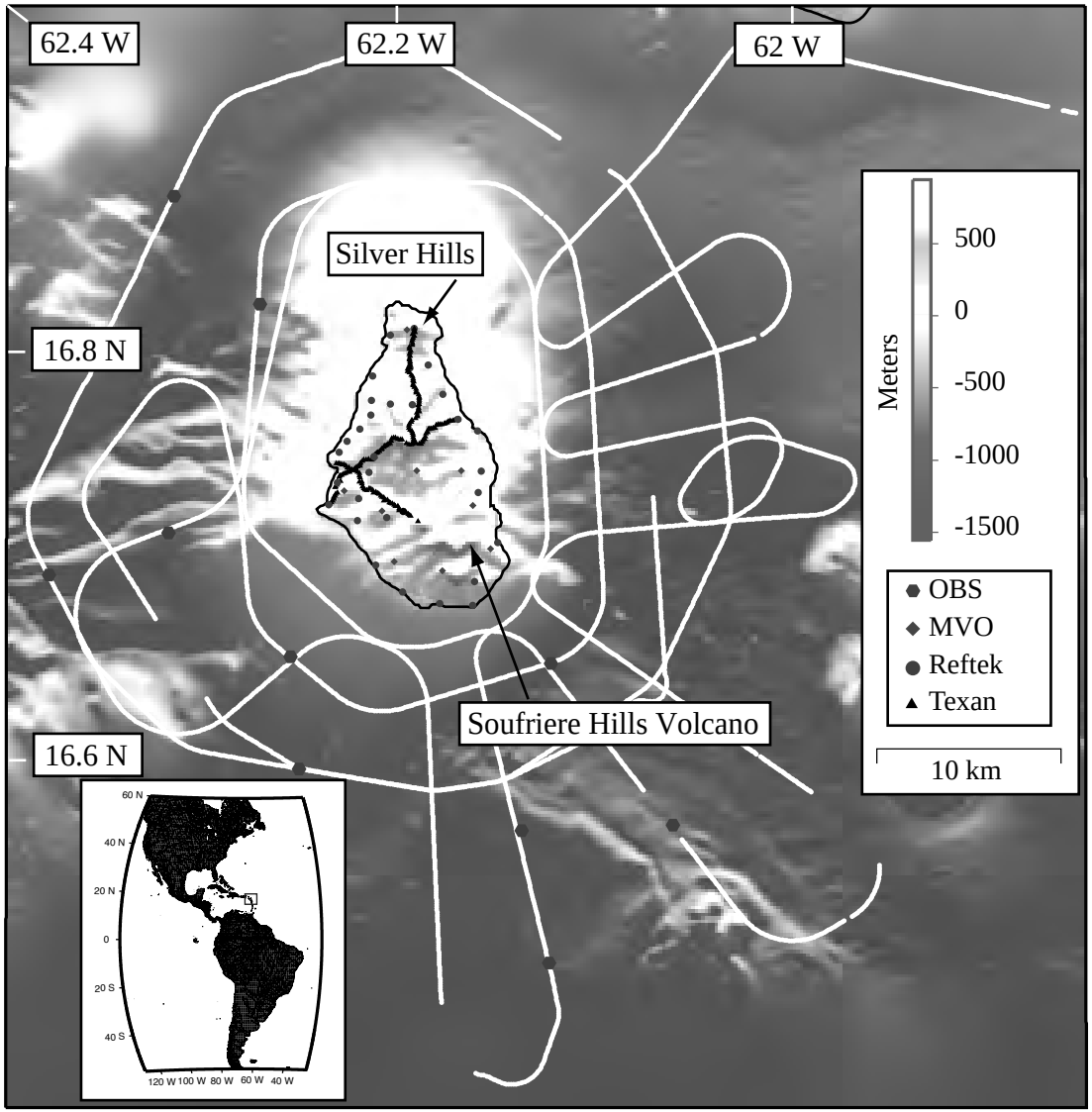

Figure 1: Montserrat is located on the eastern edge of the Caribbean plate (inset). The SEA-CALIPSO experiment included: 4402 airgun shots, white line; 10 Ocean bottom seismometers (OBS), hexagons; 10 Montserrat Volcano Obser vatory instruments (MVO), diamonds; 28 RT130 3 component recorders, circles; and 202 RT-125a single channel recorders (Texans), triangles. The Silver Hills profile runs north to south, the Centre Hills profile runs west to east, the Garibaldi profile runs southwest to northeast and the Belham Valley profile runs from northwest to south east, radial to Soufriere Hills volcano.

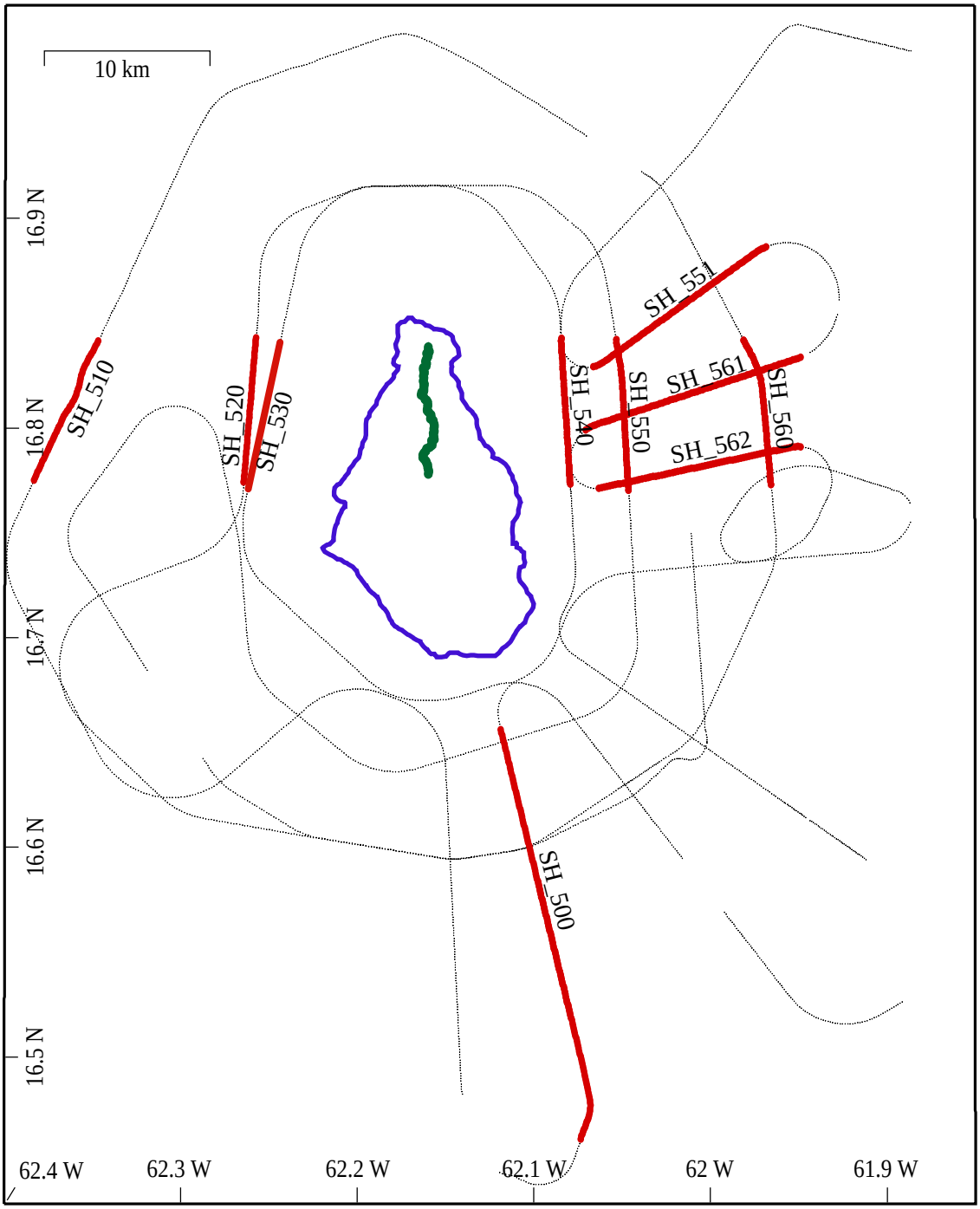

Figure 10: Silver Hills shiptracks (red) chosen because of their alignment with the Silver Hills recorders (green). East lines SH_540, SH_550, SH_551, SH_560, SH_561, SH_562 are used to study the oceanic crust east of Montserrat.

Table 3: Silver Hills RT-125a (Texan) Locations, Zone 20Q

Station Number	UTM Easting (m)	UTM Northing (m)	Elevation (m)
1	586067.9385	1852724.4402	733
2	586078.1118	1852843.9656	735
3	586071.3883	1852924.7007	731
4	586042.1466	1853038.5343	728
5	586031.0025	1853157.9731	726
6	585992.2988	1853239.6846	731
7	585951.3783	1853342.4076	741
8	585863.6145	1853431.6646	721
9	585794.9874	1853533.1691	637
10	585788.1799	1853634.9243	625
11	585834.6778	1853733.5765	574
12	585924.8519	1853837.9378	480
13	585975.6075	1853937.7140	475
14	586149.9215	1854056.8007	434
15	586259.3721	1854138.0090	410
16	586252.6075	1854228.7010	409
17	586228.6953	1854342.5562	389
18	586351.9860	1854427.1405	400
19	586339.8649	1854524.4486	376
20	586335.2766	1854604.0862	369
21	586296.3936	1854730.0499	357
22	586364.2247	1854823.2590	318
23	586341.4188	1854927.1616	313
24	586350.5547	1855038.9389	302
25	586359.7944	1855125.2709	292
26	586343.4330	1855217.0301	282
27	586313.1175	1855333.0718	273
28	586184.7982	1855437.6505	247
29	586201.5165	1855519.5876	239
30	586202.1628	1855622.4796	225
31	586078.0682	1855737.0331	229
32	586018.0088	1855829.7210	229
33	586014.5415	1855896.0871	222
34	586040.6265	1856033.3790	224
35	586031.7901	1856109.6804	221
36	586035.6342	1856212.5854	211
37	585976.5699	1856322.9788	202
38	585904.9067	1856386.8550	192
39	585829.6919	1856538.1176	184
40	585718.5767	1856607.3659	167
41	585728.7938	1856715.8284	159

Station Number	UTM Easting (m)	UTM Northing (m)	Elevation (m)
42	585841.4062	1856802.5798	169
43	585853.7135	1856921.0079	170
44	585856.5059	1857020.5897	172
45	585860.3865	1857114.6442	168
46	585824.7655	1857226.2396	160
47	585822.3331	1857300.3543	147
48	585848.5295	1857409.9882	145
49	585816.1509	1857510.5334	147
50	585841.3263	1857609.0998	166
51	585881.4204	1857707.7269	181
52	585821.2771	1857822.5416	190
53	585814.5237	1857911.0213	216
54	585963.2882	1858015.6222	259
55	585977.7790	1858120.7834	268
56	585937.9820	1858211.3412	264
57	585968.4433	1858319.8864	267
58	586022.4196	1858410.8261	273
59	586059.3009	1858512.7597	288
60	585984.2629	1858621.9815	294
61	586106.4360	1858713.1994	332
62	586077.2771	1858808.2257	374
63	586073.6157	1858922.1638	388

Table 4: Silver Hills 500 Shot Locations, Zone 20Q

FFID	Shot #	UTM Easting (m)	UTM Northing (m)	Depth (m)
2853	1877	589661.7195	1840197.9080	-791.88
2854	1878	589695.3818	1840055.3330	-801.40
2855	1879	589731.1636	1839916.0850	-813.40
2856	1880	589764.8174	1839775.7230	-822.30
2857	1881	589799.5382	1839635.3650	-822.75
2858	1882	589837.4637	1839493.9140	-830.35
2859	1883	589870.0569	1839352.4410	-834.55
2860	1884	589906.9307	1839207.6670	-837.70
2861	1885	589944.8622	1839065.1100	-845.60
2862	1886	589980.6516	1838924.7570	-845.60
2863	1887	590015.3842	1838782.1870	-847.50
2864	1888	590046.8894	1838646.2410	-846.00
2865	1889	590079.4803	1838505.8740	-853.10
2866	1890	590114.2094	1838364.4100	-857.00
2867	1891	590148.9203	1838227.3720	-860.90
2868	1892	590183.6642	1838082.5890	-860.10
2869	1893	590217.3186	1837943.3340	-864.05
2870	1894	590255.2260	1837807.4150	-870.40
2871	1895	590282.4158	1837683.6210	-869.50
2872	1896	590307.4725	1837559.8180	-877.90
2873	1897	590343.2149	1837431.6350	-880.90
2874	1898	590375.7436	1837306.7570	-883.90
2875	1899	590406.1487	1837179.6580	-901.30
2876	1900	590436.5494	1837053.6650	-908.60
2877	1901	590469.0838	1836927.6810	-911.60
2878	1902	590501.6139	1836802.8030	-912.90
2879	1903	590530.9535	1836675.6990	-922.20
2880	1904	590562.4175	1836550.8170	-919.25
2881	1905	590592.8199	1836424.8240	-926.95
2882	1906	590623.1991	1836304.3630	-933.30
2883	1907	590657.8877	1836173.9630	-933.30
2884	1908	590686.1434	1836051.2800	-925.90
2885	1909	590716.5470	1835925.2880	-906.00
2886	1910	590749.0938	1835797.0920	-907.85
2887	1911	590779.5169	1835666.6740	-918.90
2888	1912	590810.9835	1835541.7920	-919.50
2889	1913	590845.6508	1835416.9240	-927.60
2890	1914	590870.7175	1835292.0150	-935.70
2891	1915	590905.3854	1835167.1470	-935.50
2892	1916	590935.7913	1835041.1550	-936.23
2893	1917	590967.2643	1834915.1670	-940.50

FFID	Shot #	UTM Easting (m)	UTM Northing (m)	Depth (m)
2894	1918	590997.6661	1834790.2810	-937.10
2895	1919	591029.1397	1834664.2930	-931.15
2896	1920	591060.6090	1834539.4120	-925.20
2897	1921	591092.0880	1834412.3180	-921.40
2898	1922	591123.5626	1834286.3300	-921.38
2899	1923	591152.9133	1834158.1210	-922.40
2900	1924	591186.5129	1834034.3550	-908.90
2901	1925	591216.9263	1833907.2570	-896.20
2902	1926	591247.3307	1833782.3710	-896.20
2903	1927	591278.8117	1833655.2780	-893.40
2904	1928	591308.1310	1833534.8130	-897.60
2905	1929	591340.6795	1833407.7240	-897.80
2906	1930	591371.0804	1833283.9440	-895.70
2907	1931	591402.5674	1833155.7450	-897.50
2908	1932	591435.1217	1833027.5490	-898.70
2909	1933	591465.5283	1832902.6640	-901.30
2910	1934	591499.1265	1832780.0050	-901.85
2911	1935	591525.2851	1832650.6760	-904.00
2912	1936	591558.9028	1832523.5920	-903.30
2913	1937	591589.3154	1832397.6000	-913.90
2914	1938	591617.5283	1832287.0880	-917.80
2915	1939	591650.1322	1832147.8300	-921.15
2916	1940	591682.6891	1832019.6350	-922.30
2917	1941	591714.1700	1831893.6480	-926.50
2918	1942	591745.6464	1831768.7680	-930.70
2919	1943	591777.1232	1831643.8880	-934.20
2920	1944	591808.6051	1831517.9010	-936.70
2921	1945	591840.0920	1831390.8080	-935.45
2922	1946	591870.5028	1831265.9230	-933.50
2923	1947	591900.9234	1831138.8260	-936.20
2924	1948	591932.4018	1831013.9450	-936.20
2925	1949	591962.8135	1830889.0610	-940.50
2926	1950	591994.3021	1830761.9680	-941.10
2927	1951	592024.7145	1830637.0830	-937.80
2928	1952	592056.1989	1830511.0970	-941.40
2929	1953	592088.7460	1830386.2220	-951.00
2930	1954	592120.2453	1830256.9160	-955.30
2931	1955	592150.6448	1830135.3510	-959.60
2932	1956	592182.1400	1830007.1520	-961.40
2933	1957	592213.6309	1829880.0600	-963.05
2934	1958	592245.1031	1829757.3920	-966.00
2935	1959	592275.5323	1829629.1890	-964.90

FFID	Shot #	UTM Easting (m)	UTM Northing (m)	Depth (m)
2936	1960	592305.9476	1829504.3050	-966.10
2937	1961	592338.5020	1829378.3230	-967.30
2938	1962	592369.9898	1829252.3380	-973.10
2939	1963	592400.4108	1829126.3470	-975.02
2940	1964	592430.8368	1828999.2500	-976.00
2941	1965	592461.2632	1828872.1540	-980.50
2942	1966	592492.7475	1828747.2740	-982.90
2943	1967	592523.1602	1828623.4960	-982.90
2944	1968	592553.5781	1828498.6120	-984.50
2945	1969	592586.1447	1828370.4190	-988.20
2946	1970	592618.6974	1828245.5440	-988.20
2947	1971	592648.0443	1828121.7620	-989.40
2948	1972	592680.6072	1827994.6750	-993.10
2949	1973	592712.1033	1827867.5830	-994.85
2950	1974	592743.5950	1827741.5980	-993.30
2951	1975	592775.0918	1827614.5060	-994.30
2952	1976	592805.5074	1827490.7290	-995.30
2953	1977	592837.0000	1827364.7430	-996.30
2954	1978	592868.4930	1827238.7580	-999.40
2955	1979	592898.9191	1827112.7680	-1000.05
2956	1980	592930.4128	1826986.7830	-997.20
2957	1981	592961.9019	1826861.9040	-996.10
2958	1982	592993.4058	1826733.7060	-996.80
2959	1983	593022.7612	1826608.8180	-997.50
2960	1984	593056.3953	1826481.7360	-997.50
2961	1985	593086.8138	1826357.9590	-998.10
2962	1986	593118.3094	1826231.9740	-996.80
2963	1987	593149.8053	1826105.9890	-997.50
2964	1988	593181.3064	1825978.8980	-1001.40
2965	1989	593210.6636	1825854.0110	-1001.40
2966	1990	593243.2278	1825728.0300	-1002.40
2967	1991	593273.6434	1825605.3600	-1002.60
2968	1992	593305.1505	1825477.1630	-1002.40
2969	1993	593336.6532	1825350.0720	-1001.70
2970	1994	593368.1466	1825225.1930	-1001.80
2971	1995	593398.5778	1825099.2040	-1002.30
2972	1996	593430.0815	1824972.1130	-1002.80
2973	1997	593461.5759	1824847.2350	-1004.15
2974	1998	593494.1379	1824722.3620	-1003.85
2975	1999	593524.5704	1824596.3730	-1004.70
2976	2000	593556.0610	1824472.6010	-1005.50
2977	2001	593587.5662	1824345.5100	-1005.50

FFID	Shot #	UTM Easting (m)	UTM Northing (m)	Depth (m)
2978	2002	593619.0574	1824221.7390	-1005.50
2979	2003	593649.5009	1824093.5370	-1005.50
2980	2004	593680.9975	1823968.6590	-1005.50
2981	2005	593710.3502	1823845.9850	-1005.50
2982	2006	593742.9341	1823716.6860	-1005.50
2983	2007	593770.1719	1823589.5770	-1005.50
2984	2008	593795.2752	1823462.4590	-1005.50
2985	2009	593821.4414	1823336.4520	-1005.50
2986	2010	593847.6175	1823208.2320	-1005.50
2987	2011	593871.6494	1823082.2160	-1005.50
2988	2012	593898.8885	1822955.1070	-1005.50
2989	2013	593925.0413	1822832.4190	-1005.50
2990	2014	593950.1558	1822703.0880	-1005.50
2991	2015	593976.3380	1822573.7620	-1005.50
2992	2016	594002.5060	1822447.7550	-1005.50
2993	2017	594029.7514	1822319.5400	-1005.50
2994	2018	594055.9247	1822192.4270	-1005.50
2995	2019	594079.9587	1822066.4100	-1005.50
2996	2020	594099.7327	1821938.1630	-1005.50
2997	2021	594106.6927	1821810.9660	-1005.50
2998	2022	594102.9974	1821679.2970	-1005.50
2999	2023	594090.7286	1821555.3350	-1005.50
3000	2024	594066.7463	1821424.6840	-1005.50
3001	2025	594036.2817	1821311.7060	-1005.50
3002	2026	594003.6335	1821209.7820	-1005.50
3003	2027	593972.0139	1821116.7130	-1005.50
3004	2028	593939.3266	1821023.6390	-1005.50
3005	2029	593905.5714	1820930.5610	-1005.50
3006	2030	593873.9269	1820843.0240	-1005.50
3007	2031	593838.0265	1820752.1490	-1005.50
3008	2032	593803.1788	1820664.5980	-1005.50
3009	2033	593768.3357	1820575.9400	-1005.50
3010	2034	593733.4827	1820489.4960	-1005.50
3011	2035	593699.6920	1820404.1620	-1005.50
3012	2036	593664.8912	1820305.5480	-1005.50
3013	2037	593625.9591	1820174.8330	-1005.50

Table 5: Silver Hills 510 Shot Locations, Zone 20Q

FFID	Shot #	UTM Easting (m)	UTM Northing (m)	Depth (m)
3438	2462	566483.3231	1852410.5300	-1116.10
3439	2463	566545.7957	1852542.3750	-1115.70
3440	2464	566607.2050	1852673.1100	-1107.30
3441	2465	566666.4784	1852804.9450	-1107.30
3442	2466	566730.0214	1852934.5810	-1096.90
3443	2467	566792.4908	1853066.4260	-1079.70
3444	2468	566854.9663	1853196.0600	-1074.15
3445	2469	566917.4340	1853327.9060	-1065.20
3446	2470	566978.8387	1853458.6420	-1047.40
3447	2471	567042.3776	1853588.2790	-1039.10
3448	2472	567104.8465	1853719.0200	-1029.60
3449	2473	567166.2452	1853850.8630	-1014.90
3450	2474	567228.7055	1853983.8160	-1000.65
3451	2475	567291.1719	1854114.5570	-992.15
3452	2476	567351.5096	1854244.1860	-984.50
3453	2477	567415.0261	1854379.3560	-967.10
3454	2478	567472.1755	1854505.6550	-961.40
3455	2479	567536.7632	1854638.6160	-952.50
3456	2480	567600.2915	1854769.3620	-937.45
3457	2481	567662.7602	1854897.8920	-921.10
3458	2482	567727.3526	1855028.6410	-921.10
3459	2483	567789.8162	1855158.2780	-907.70
3460	2484	567851.2027	1855291.2300	-889.40
3461	2485	567912.5990	1855420.8640	-879.10
3462	2486	567975.0567	1855551.6070	-873.60
3463	2487	568041.7799	1855681.2580	-850.30
3464	2488	568126.6798	1855792.1610	-838.00
3465	2489	568204.1475	1855894.1900	-829.30
3466	2490	568275.2096	1855999.5180	-809.70
3467	2491	568343.0560	1856110.3670	-812.10
3468	2492	568410.8838	1856226.7470	-786.10
3469	2493	568470.1783	1856345.3130	-776.38
3470	2494	568527.3300	1856467.1910	-765.40
3471	2495	568581.2697	1856593.4840	-740.40
3472	2496	568630.9353	1856723.0820	-731.07
3473	2497	568677.3926	1856855.9880	-722.40
3474	2498	568716.3862	1856989.9770	-695.40
3475	2499	568751.1203	1857122.8460	-665.00
3476	2500	568779.4422	1857261.2260	-649.65
3477	2501	568810.9677	1857397.4030	-637.30
3478	2502	568844.6384	1857529.1620	-612.00

FFID	Shot #	UTM Easting (m)	UTM Northing (m)	Depth (m)
3479	2503	568887.9100	1857657.6340	-590.60
3480	2504	568932.2430	1857787.2160	-590.60
3481	2505	568985.1110	1857913.5070	-567.50
3482	2506	569040.1276	1858034.2730	-540.20
3483	2507	569099.4023	1858156.1600	-540.20
3484	2508	569161.8802	1858275.8450	-517.35
3485	2509	569229.6925	1858393.3350	-513.90
3486	2510	569297.4968	1858513.0380	-513.90
3487	2511	569365.3039	1858631.6350	-559.90
3488	2512	569430.9755	1858751.3310	-563.40
3489	2513	569492.3841	1858871.0140	-566.90
3490	2514	569558.0542	1858990.7110	-611.50
3491	2515	569623.7198	1859111.5140	-614.60
3492	2516	569688.3192	1859232.3140	-636.20

Table 6: Silver Hills 520 Shot Locations, Zone 20Q

FFID	Shot #	UTM Easting (m)	UTM Northing (m)	Depth (m)
4352	3376	576905.9130	1852317.4720	-626.40
4353	3377	576920.3213	1852459.1320	-618.60
4354	3378	576932.6016	1852599.6780	-617.30
4355	3379	576944.8978	1852735.7990	-617.50
4356	3380	576956.1320	1852870.8100	-621.65
4357	3381	576967.3539	1853009.1400	-625.80
4358	3382	576978.5796	1853146.3630	-640.70
4359	3383	576989.7972	1853285.7990	-653.50
4360	3384	577002.0843	1853424.1330	-662.63
4361	3385	577014.3713	1853562.4670	-671.75
4362	3386	577028.7776	1853704.1270	-677.80
4363	3387	577041.0602	1853843.5680	-692.10
4364	3388	577053.3586	1853978.5830	-701.10
4365	3389	577063.5172	1854115.8020	-710.10
4366	3390	577072.6098	1854253.0180	-732.20
4367	3391	577082.7680	1854390.2380	-755.30
4368	3392	577093.9838	1854529.6750	-761.80
4369	3393	577107.3309	1854669.1190	-768.30
4370	3394	577121.7355	1854810.7800	-780.90
4371	3395	577135.0742	1854952.4370	-790.00
4372	3396	577149.5025	1855087.4600	-794.75
4373	3397	577162.8487	1855226.9040	-794.30
4374	3398	577175.1452	1855361.9190	-804.35
4375	3399	577185.3099	1855496.9270	-807.65
4376	3400	577197.5939	1855635.2610	-803.55
4377	3401	577205.5905	1855780.2180	-809.00
4378	3402	577210.4262	1855915.2060	-805.50
4379	3403	577220.5863	1856051.3200	-814.30
4380	3404	577238.2505	1856175.2920	-816.40
4381	3405	577249.5042	1856303.6650	-818.50
4382	3406	577262.9214	1856423.1970	-816.40
4383	3407	577272.0717	1856543.8190	-818.60
4384	3408	577283.3411	1856667.7670	-820.80
4385	3409	577293.5446	1856791.7120	-807.20
4386	3410	577303.7439	1856916.7630	-807.60
4387	3411	577311.8239	1857038.4870	-808.00
4388	3412	577322.0310	1857161.3260	-808.70
4389	3413	577333.2996	1857285.2750	-801.92
4390	3414	577341.3751	1857408.1060	-796.15
4391	3415	577352.6474	1857530.9480	-792.15
4392	3416	577363.9236	1857652.6840	-786.40

FFID	Shot #	UTM Easting (m)	UTM Northing (m)	Depth (m)
4393	3417	577374.1259	1857776.6290	-784.10
4394	3418	577385.3977	1857899.4720	-784.60
4395	3419	577394.5382	1858022.3070	-785.60
4396	3420	577406.8752	1858145.1530	-786.60
4397	3421	577416.0073	1858270.2010	-794.30
4398	3422	577427.2865	1858390.8310	-796.65
4399	3423	577438.5575	1858513.6730	-799.00
4400	3424	577448.7588	1858637.6190	-799.80
4401	3425	577456.8327	1858760.4500	-799.95
4402	3426	577467.0539	1858878.8630	-800.10
4403	3427	577479.3614	1859009.4540	-802.20
4404	3428	577491.6809	1859136.7260	-801.90
4405	3429	577501.9261	1859248.5020	-796.85
4406	3430	577507.8520	1859375.7510	-797.55

Table 7: Silver Hills 530 Shot Locations, Zone 20Q

FFID	Shot #	UTM Easting (m)	UTM Northing (m)	Depth (m)
2910	1934	591499.1265	1832780.0050	-901.85
2911	1935	591525.2851	1832650.6760	-904.00
2912	1936	591558.9028	1832523.5920	-903.30
2913	1937	591589.3154	1832397.6000	-913.90
2914	1938	591617.5283	1832287.0880	-917.80
2915	1939	591650.1322	1832147.8300	-921.15
2916	1940	591682.6891	1832019.6350	-922.30
2917	1941	591714.1700	1831893.6480	-926.50
2918	1942	591745.6464	1831768.7680	-930.70
2919	1943	591777.1232	1831643.8880	-934.20
2920	1944	591808.6051	1831517.9010	-936.70
2921	1945	591840.0920	1831390.8080	-935.45
2922	1946	591870.5028	1831265.9230	-933.50
2923	1947	591900.9234	1831138.8260	-936.20
2924	1948	591932.4018	1831013.9450	-936.20
2925	1949	591962.8135	1830889.0610	-940.50
2926	1950	591994.3021	1830761.9680	-941.10
2927	1951	592024.7145	1830637.0830	-937.80
2928	1952	592056.1989	1830511.0970	-941.40
2929	1953	592088.7460	1830386.2220	-951.00
2930	1954	592120.2453	1830256.9160	-955.30
2931	1955	592150.6448	1830135.3510	-959.60
2932	1956	592182.1400	1830007.1520	-961.40
2933	1957	592213.6309	1829880.0600	-963.05
2934	1958	592245.1031	1829757.3920	-966.00
2935	1959	592275.5323	1829629.1890	-964.90
2936	1960	592305.9476	1829504.3050	-966.10
2937	1961	592338.5020	1829378.3230	-967.30
2938	1962	592369.9898	1829252.3380	-973.10
2939	1963	592400.4108	1829126.3470	-975.02
2940	1964	592430.8368	1828999.2500	-976.00
2941	1965	592461.2632	1828872.1540	-980.50
2942	1966	592492.7475	1828747.2740	-982.90
2943	1967	592523.1602	1828623.4960	-982.90
2944	1968	592553.5781	1828498.6120	-984.50
2945	1969	592586.1447	1828370.4190	-988.20
2946	1970	592618.6974	1828245.5440	-988.20
2947	1971	592648.0443	1828121.7620	-989.40
2948	1972	592680.6072	1827994.6750	-993.10
2949	1973	592712.1033	1827867.5830	-994.85
2950	1974	592743.5950	1827741.5980	-993.30

FFID	Shot #	UTM Easting (m)	UTM Northing (m)	Depth (m)
2951	1975	592775.0918	1827614.5060	-994.30
2952	1976	592805.5074	1827490.7290	-995.30
2953	1977	592837.0000	1827364.7430	-996.30
2954	1978	592868.4930	1827238.7580	-999.40
2955	1979	592898.9191	1827112.7680	-1000.05
2956	1980	592930.4128	1826986.7830	-997.20
2957	1981	592961.9019	1826861.9040	-996.10
2958	1982	592993.4058	1826733.7060	-996.80
2959	1983	593022.7612	1826608.8180	-997.50
2960	1984	593056.3953	1826481.7360	-997.50
2961	1985	593086.8138	1826357.9590	-998.10
2962	1986	593118.3094	1826231.9740	-996.80
2963	1987	593149.8053	1826105.9890	-997.50

Table 8: Silver Hills 540 Shot Locations, Zone 20Q

FFID	Shot #	UTM Easting (m)	UTM Northing (m)	Depth (m)
1285	309	592663.5078	1859362.7390	-571.40
1286	310	592660.9183	1859224.4320	-571.40
1287	311	592666.8486	1859087.2700	-568.60
1288	312	592673.8445	1858950.1120	-569.80
1289	313	592681.9157	1858810.7470	-569.40
1290	314	592689.9870	1858671.3810	-569.40
1291	315	592696.9831	1858534.2240	-569.10
1292	316	592708.2513	1858394.8720	-566.90
1293	317	592718.4541	1858255.5160	-562.00
1294	318	592726.5207	1858117.2570	-562.00
1295	319	592734.5875	1857978.9970	-561.30
1296	320	592743.7199	1857840.7430	-552.90
1297	321	592752.8670	1857699.1690	-545.00
1298	322	592761.9899	1857563.1280	-545.00
1299	323	592770.0569	1857424.8680	-534.90
1300	324	592779.1896	1857286.6140	-529.70
1301	325	592787.2567	1857148.3550	-537.65
1302	326	592796.4041	1857006.7810	-533.60
1303	327	592804.4664	1856869.6290	-529.55
1304	328	592811.4680	1856731.3650	-523.60
1305	329	592820.6156	1856589.7920	-532.70
1306	330	592829.7438	1856452.6440	-528.80
1307	331	592837.8209	1856312.1720	-524.90
1308	332	592846.9347	1856178.3430	-516.70
1309	333	592855.0120	1856037.8710	-512.60
1310	334	592865.2159	1855898.5150	-509.70
1311	335	592874.3396	1855762.4740	-506.80
1312	336	592885.6046	1855624.2290	-497.90
1313	337	592904.3204	1855488.2290	-494.10
1314	338	592910.2567	1855349.9610	-494.10
1315	339	592920.4611	1855210.6050	-488.00
1316	340	592928.5292	1855072.3460	-480.80
1317	341	592938.7386	1854931.8840	-473.10
1318	342	592946.8018	1854794.7310	-468.95
1319	343	592955.9359	1854656.4770	-464.80
1320	344	592961.8628	1854520.4220	-461.60
1321	345	592969.9457	1854378.8440	-480.45
1322	346	592981.2212	1854238.3860	-477.40
1323	347	592991.4262	1854099.0310	-474.35
1324	348	592997.3582	1853961.8690	-462.25
1325	349	593005.4316	1853822.5040	-451.45

FFID	Shot #	UTM Easting (m)	UTM Northing (m)	Depth (m)
1326	350	593016.7026	1853683.1530	-466.10
1327	351	593024.7567	1853548.2130	-462.40
1328	352	593032.8448	1853405.5290	-454.50
1329	353	593041.9746	1853268.3810	-455.70
1330	354	593052.1947	1853125.7070	-454.35
1331	355	593059.1734	1852992.9750	-453.00
1332	356	593063.8064	1852908.9120	-443.90
1333	357	593065.3439	1852801.6030	-443.90
1334	358	593068.9694	1852704.2600	-423.70
1335	359	593078.9466	1852616.9020	-423.70
1336	360	593085.7748	1852518.4660	-421.60
1337	361	593092.5738	1852426.6690	-421.60
1338	362	593098.2923	1852338.1860	-423.20
1339	363	593101.9228	1852239.7370	-423.20

Table 9: Silver Hills 550 Shot Locations, Zone 20Q

FFID	Shot #	UTM Easting (m)	UTM Northing (m)	Depth (m)
4608	3632	595387.5290	1859283.0480	-759.30
4609	3633	595405.1635	1859153.6830	-758.60
4610	3634	595429.2117	1859019.9220	-757.85
4611	3635	595452.1896	1858887.2620	-760.70
4612	3636	595478.3546	1858756.8290	-764.20
4613	3637	595496.0099	1858623.0390	-763.10
4614	3638	595513.6654	1858489.2480	-763.50
4615	3639	595535.5786	1858356.5840	-763.90
4616	3640	595568.1183	1858230.6050	-765.10
4617	3641	595592.1633	1858097.9500	-765.80
4618	3642	595608.7540	1857964.1550	-766.50
4619	3643	595625.3399	1857831.4670	-774.55
4620	3644	595636.5976	1857698.7540	-775.05
4621	3645	595654.2444	1857567.1760	-776.13
4622	3646	595669.7651	1857434.4830	-779.30
4623	3647	595676.7554	1857302.8570	-784.50
4624	3648	595685.8821	1857170.1350	-790.45
4625	3649	595695.0190	1857035.2000	-796.40
4626	3650	595706.2722	1856903.5930	-813.30
4627	3651	595716.4699	1856769.7690	-820.10
4628	3652	595722.3998	1856637.0320	-821.90
4629	3653	595724.0768	1856502.0640	-823.70
4630	3654	595728.9560	1856366.0030	-826.60
4631	3655	595740.2247	1856231.0780	-830.70
4632	3656	595755.7363	1856100.5970	-830.70
4633	3657	595761.6814	1855964.5410	-836.10
4634	3658	595764.4142	1855831.7900	-836.10
4635	3659	595770.3493	1855697.9470	-848.20
4636	3660	595779.4718	1855566.3310	-848.20
4637	3661	595790.7458	1855430.2990	-850.70
4638	3662	595799.8834	1855295.3640	-850.10
4639	3663	595807.9603	1855159.3180	-856.68
4640	3664	595812.8198	1855027.6830	-856.45
4641	3665	595819.8210	1854893.8450	-853.30
4642	3666	595827.8930	1854758.9050	-851.75
4643	3667	595840.2133	1854627.3040	-851.75
4644	3668	595846.1538	1854492.3550	-848.80
4645	3669	595851.0284	1854357.4010	-855.80
4646	3670	595852.6956	1854224.6450	-857.10
4647	3671	595868.2237	1854090.8450	-858.40
4648	3672	595876.2960	1853955.9060	-856.90

FFID	Shot #	UTM Easting (m)	UTM Northing (m)	Depth (m)
4649	3673	595886.5001	1853820.9760	-856.20
4650	3674	595895.6334	1853687.1470	-857.05
4651	3675	595897.3056	1853553.2850	-857.90
4652	3676	595898.9929	1853416.1040	-857.30
4653	3677	595911.3189	1853283.3960	-857.00
4654	3678	595924.7210	1853148.4810	-857.90
4655	3679	595939.1840	1853014.6770	-858.80
4656	3680	595944.0591	1852879.7230	-860.80
4657	3681	595945.7364	1852744.7550	-864.10
4658	3682	595948.4796	1852609.7910	-867.40
4659	3683	595959.7452	1852475.9720	-870.80
4660	3684	595973.1528	1852339.9510	-870.60
4661	3685	595982.2817	1852207.2290	-871.10
4662	3686	595988.2279	1852071.1730	-871.60
4663	3687	595990.9662	1851937.3160	-874.70

Table 10: Silver Hills 551 Shot Locations, Zone 20Q

FFID	Shot #	UTM Easting (m)	UTM Northing (m)	Depth (m)
2170	1194	594258.5448	1857965.8300	-705.70
2171	1195	594387.3247	1858002.9150	-711.10
2172	1196	594516.0448	1858053.2770	-716.50
2173	1197	594640.4273	1858120.2160	-725.00
2174	1198	594754.1229	1858193.7460	-728.95
2175	1199	594867.7880	1858273.9140	-732.55
2176	1200	594979.3209	1858354.0740	-740.00
2177	1201	595095.1105	1858435.3600	-744.45
2178	1202	595206.6417	1858515.5210	-747.10
2179	1203	595322.4346	1858595.7010	-755.40
2180	1204	595432.9086	1858673.6460	-755.85
2181	1205	595546.5685	1858753.8190	-764.20
2182	1206	595660.2327	1858832.8850	-772.90
2183	1207	595774.9465	1858915.2770	-773.30
2184	1208	595887.5434	1858994.3400	-779.80
2185	1209	596001.2100	1859072.3020	-782.95
2186	1210	596115.9313	1859152.4830	-786.60
2187	1211	596225.3239	1859232.6400	-792.05
2188	1212	596337.9174	1859311.7060	-794.10
2189	1213	596456.8833	1859395.2270	-796.40
2190	1214	596568.4045	1859475.3960	-800.60
2191	1215	596683.1114	1859557.7920	-802.00
2192	1216	596795.6813	1859641.2860	-804.20
2193	1217	596904.0134	1859719.2290	-806.60
2194	1218	597015.5312	1859799.4010	-806.10
2195	1219	597131.3002	1859881.8050	-808.90
2196	1220	597248.1339	1859964.2150	-810.35
2197	1221	597355.3768	1860046.5810	-809.70
2198	1222	597471.1636	1860124.5620	-810.60
2199	1223	597582.6926	1860201.4170	-809.25
2200	1224	597698.4675	1860281.6120	-809.70
2201	1225	597811.0501	1860360.6860	-809.10
2202	1226	597922.5561	1860441.9690	-809.35
2203	1227	598039.3837	1860524.3840	-808.35
2204	1228	598150.8982	1860603.4550	-808.30
2205	1229	598265.5982	1860684.7550	-807.60
2206	1230	598381.3628	1860766.0600	-807.50
2207	1231	598487.5473	1860845.1080	-806.70
2208	1232	598604.3809	1860925.3130	-807.00
2209	1233	598718.0171	1861005.5040	-807.00
2210	1234	598831.6525	1861085.6960	-805.02

FFID	Shot #	UTM Easting (m)	UTM Northing (m)	Depth (m)
2211	1235	598944.2319	1861163.6710	-804.40
2212	1236	599056.7949	1861244.9650	-801.85
2213	1237	599170.4278	1861325.1580	-801.40
2214	1238	599287.2406	1861408.6870	-802.80
2215	1239	599402.9974	1861489.9980	-801.70
2216	1240	599524.0599	1861575.7610	-801.65
2217	1241	599639.8149	1861657.0730	-800.30
2218	1242	599749.1868	1861736.1440	-799.70
2219	1243	599860.6520	1861822.9690	-798.35
2220	1244	599960.4803	1861892.0380	-796.90
2221	1245	600063.4938	1861963.3360	-797.15
2222	1246	600165.4464	1862033.5220	-795.40
2223	1247	600269.5135	1862107.0390	-794.20
2224	1248	600369.3391	1862176.1100	-793.45
2225	1249	600471.2739	1862249.6170	-792.00
2226	1250	600567.9071	1862317.5670	-792.00
2227	1251	600674.0918	1862393.3090	-789.40
2228	1252	600772.8493	1862462.3770	-789.80
2229	1253	600872.6558	1862534.7690	-790.20
2230	1254	600974.5818	1862609.3860	-788.50
2231	1255	601073.3428	1862677.3490	-788.50
2232	1256	601176.3382	1862750.8650	-787.45
2233	1257	601277.2180	1862821.0520	-786.70
2234	1258	601378.0865	1862893.4530	-786.10
2235	1259	601476.8235	1862965.8430	-784.25
2236	1260	601581.9630	1863036.0530	-784.10
2237	1261	601680.7093	1863106.2320	-784.00
2238	1262	601780.5097	1863178.6290	-783.60
2239	1263	601881.3695	1863252.1380	-783.90
2240	1264	601982.2500	1863321.2230	-781.60
2241	1265	602084.1738	1863394.7390	-781.70
2242	1266	602181.8461	1863466.0210	-781.70
2243	1267	602282.7301	1863534.0010	-779.80
2244	1268	602382.5265	1863606.4020	-781.30
2245	1269	602491.9429	1863672.2110	-780.55
2246	1270	602602.4510	1863732.4950	-780.30
2247	1271	602709.7894	1863787.2310	-780.10
2248	1272	602821.3887	1863841.9890	-779.80

Table 11: Silver Hills 560 Shot Locations, 20Q

FFID	Shot #	UTM Easting (m)	UTM Northing (m)	Depth (m)
3828	2852	601713.0716	1859269.4410	-824.10
3829	2853	601770.0711	1859161.2900	-825.70
3830	2854	601829.2078	1859052.0430	-826.40
3831	2855	601888.3398	1858943.9030	-826.80
3832	2856	601946.4067	1858835.7570	-828.70
3833	2857	602005.5505	1858725.4050	-828.70
3834	2858	602071.1529	1858601.8070	-830.10
3835	2859	602137.8056	1858481.5330	-832.60
3836	2860	602203.4041	1858359.0420	-832.05
3837	2861	602264.7567	1858233.2110	-834.40
3838	2862	602321.8421	1858108.4660	-836.50
3839	2863	602372.5449	1857981.4780	-836.00
3840	2864	602423.2697	1857850.0640	-837.70
3841	2865	602467.6117	1857716.4060	-840.00
3842	2866	602506.6097	1857586.0420	-840.90
3843	2867	602540.3012	1857451.2270	-841.80
3844	2868	602569.7302	1857316.3900	-843.50
3845	2869	602595.9732	1857179.3260	-846.20
3846	2870	602616.8879	1857042.2360	-847.45
3847	2871	602634.6111	1856904.0240	-848.70
3848	2872	602647.0058	1856765.7860	-850.70
3849	2873	602660.4609	1856628.6600	-851.40
3850	2874	602671.7901	1856490.4170	-852.35
3851	2875	602685.2562	1856351.0780	-853.30
3852	2876	602696.5802	1856213.9410	-853.90
3853	2877	602712.1727	1856075.7190	-856.00
3854	2878	602724.5787	1855935.2680	-856.65
3855	2879	602739.1057	1855797.0410	-857.25
3856	2880	602751.4959	1855659.9090	-858.15
3857	2881	602763.8916	1855521.6720	-859.95
3858	2882	602777.3370	1855386.7580	-860.75
3859	2883	602790.8363	1855240.7810	-861.10
3860	2884	602807.4741	1855106.9900	-859.00
3861	2885	602814.5357	1854969.8320	-861.20
3862	2886	602828.0031	1854830.4940	-861.55
3863	2887	602841.4706	1854691.1550	-861.90
3864	2888	602853.8509	1854556.2360	-863.30
3865	2889	602864.1265	1854415.7750	-864.90
3866	2890	602878.6602	1854276.4420	-865.40
3867	2891	602889.9911	1854138.1990	-865.90
3868	2892	602905.5909	1853998.8710	-867.70

FFID	Shot #	UTM Easting (m)	UTM Northing (m)	Depth (m)
3869	2893	602916.9058	1853863.9470	-868.60
3870	2894	602929.3136	1853723.4970	-868.60
3871	2895	602942.7821	1853584.1580	-868.95
3872	2896	602956.2399	1853447.0320	-870.95
3873	2897	602967.5660	1853309.8960	-871.40
3874	2898	602979.9688	1853170.5520	-872.10
3875	2899	602994.4982	1853032.3250	-872.80
3876	2900	603006.8906	1852895.1940	-875.60
3877	2901	603020.3543	1852756.9610	-878.60
3878	2902	603031.6755	1852620.9320	-879.80
3879	2903	603044.0789	1852481.5880	-881.00
3880	2904	603058.6090	1852343.3610	-885.00
3881	2905	603071.0126	1852204.0170	-888.50

Table 12: Silver Hills 561 Shot Locations, Zone 20Q

FFID	Shot #	UTM Easting (m)	UTM Northing (m)	Depth (m)
2312	1336	604544.2999	1858437.9930	-816.40
2313	1337	604415.6027	1858387.5690	-817.80
2314	1338	604287.9378	1858343.7880	-820.50
2315	1339	604153.8840	1858298.8710	-821.55
2316	1340	604023.0157	1858256.1830	-822.10
2317	1341	603893.2180	1858212.3950	-823.40
2318	1342	603758.0915	1858168.5810	-825.00
2319	1343	603626.1506	1858126.9970	-827.05
2320	1344	603494.2147	1858084.3070	-827.90
2321	1345	603363.3439	1858041.6230	-828.90
2322	1346	603230.3413	1857998.9300	-830.60
2323	1347	603096.2780	1857955.1260	-832.20
2324	1348	602964.3347	1857913.5460	-833.60
2325	1349	602833.4674	1857869.7590	-834.70
2326	1350	602701.5231	1857828.1810	-836.00
2327	1351	602568.5235	1857784.3860	-838.00
2328	1352	602435.5233	1857740.5910	-840.00
2329	1353	602303.5776	1857699.0150	-841.00
2330	1354	602171.6314	1857657.4400	-841.70
2331	1355	602036.5037	1857612.5320	-842.35
2332	1356	601907.7536	1857570.9740	-844.40
2333	1357	601775.8166	1857527.1890	-846.60
2334	1358	601643.8578	1857487.8300	-848.00
2335	1359	601510.8541	1857444.0420	-848.35
2336	1360	601376.7896	1857399.1430	-850.10
2337	1361	601248.0424	1857356.4830	-852.90
2338	1362	601112.9005	1857313.7930	-853.80
2339	1363	600978.8027	1857275.5350	-854.10
2340	1364	600849.0095	1857228.4470	-855.85
2341	1365	600718.1289	1857185.7800	-857.60
2342	1366	600585.1217	1857141.9980	-858.90
2343	1367	600452.1088	1857099.3220	-858.85
2344	1368	600320.1505	1857058.8660	-858.80
2345	1369	600189.2733	1857015.0960	-859.80
2346	1370	600054.1431	1856969.0940	-863.20
2347	1371	599925.3701	1856930.8680	-863.20
2348	1372	599792.3652	1856885.9850	-864.60
2349	1373	599660.4150	1856843.3200	-865.10
2350	1374	599528.4695	1856799.5490	-867.60
2351	1375	599394.3817	1856757.9820	-867.60
2352	1376	599266.6877	1856716.4460	-868.20

FFID	Shot #	UTM Easting (m)	UTM Northing (m)	Depth (m)
2353	1377	599131.5332	1856674.8760	-868.20
2354	1378	598999.5857	1856631.1090	-872.15
2355	1379	598868.6983	1856588.4540	-876.10
2356	1380	598735.6790	1856545.7900	-878.10
2357	1381	598604.7906	1856503.1370	-879.90
2358	1382	598470.7096	1856459.3630	-886.50
2359	1383	598338.7597	1856415.6000	-892.80
2360	1384	598203.5812	1856378.4620	-893.10
2361	1385	598074.8377	1856332.5030	-894.90
2362	1386	597943.9469	1856289.8540	-900.05
2363	1387	597810.9343	1856244.9830	-905.00
2364	1388	597680.0527	1856200.1230	-909.60
2365	1389	597549.1604	1856157.4770	-912.00
2366	1390	597416.1360	1856114.8210	-912.20
2367	1391	597284.1770	1856072.1710	-912.25
2368	1392	597152.2174	1856029.5230	-910.50
2369	1393	597020.2624	1855985.7680	-905.70
2370	1394	596886.1501	1855947.5370	-902.10
2371	1395	596756.3459	1855899.3690	-900.00
2372	1396	596624.3743	1855858.9360	-893.70
2373	1397	596492.4173	1855815.1850	-885.60
2374	1398	596359.3840	1855773.6430	-881.70
2375	1399	596226.3603	1855729.8890	-879.10
2376	1400	596094.3968	1855687.2470	-871.10
2377	1401	595962.4277	1855645.7120	-863.70
2378	1402	595833.6606	1855603.0860	-855.95
2379	1403	595703.8271	1855560.4570	-848.20
2380	1404	595568.6694	1855516.6970	-834.35
2381	1405	595437.7692	1855474.0640	-820.20
2382	1406	595302.6104	1855430.3070	-812.75
2383	1407	595169.5727	1855388.7720	-805.30
2384	1408	595038.6710	1855346.1420	-789.55
2385	1409	594910.9563	1855305.7390	-770.00
2386	1410	594789.6308	1855266.4730	-770.00
2387	1411	594669.3708	1855227.2110	-749.70
2388	1412	594508.6697	1855174.4940	-730.10
2389	1413	594377.7705	1855130.7610	-708.30
2390	1414	594247.9563	1855082.6090	-708.30
2391	1415	594121.3882	1855023.4090	-686.80
2392	1416	594000.1877	1854955.3820	-662.90
2393	1417	593887.5227	1854885.1810	-649.05

Table 13: Silver Hills 562 Shot Locations, Zone 20Q

FFID	Shot #	UTM Easting (m)	UTM Northing (m)	Depth (m)
2422	1446	594518.4580	1852026.9500	-739.60
2423	1447	594653.7342	1852049.6810	-762.90
2424	1448	594788.9854	1852077.9450	-774.05
2425	1449	594925.3071	1852105.1070	-785.20
2426	1450	595060.5577	1852133.3730	-803.00
2427	1451	595194.7420	1852161.6340	-820.00
2428	1452	595331.0629	1852188.8000	-835.20
2429	1453	595467.3684	1852219.2850	-842.82
2430	1454	595601.5568	1852246.4430	-849.30
2431	1455	595739.9986	1852275.8330	-860.60
2432	1456	595875.2522	1852302.9980	-870.60
2433	1457	596011.5615	1852332.3800	-874.75
2434	1458	596146.7794	1852367.2910	-878.90
2435	1459	596285.2500	1852390.0470	-886.40
2436	1460	596419.4264	1852419.4220	-891.80
2437	1461	596553.6176	1852445.4800	-895.65
2438	1462	596690.9912	1852474.8720	-899.50
2439	1463	596829.4354	1852503.1630	-908.10
2440	1464	596964.6765	1852532.5470	-914.20
2441	1465	597098.8310	1852566.3530	-912.25
2442	1466	597231.9750	1852587.9840	-912.25
2443	1467	597369.3470	1852617.3810	-916.20
2444	1468	597505.6577	1852645.6670	-915.70
2445	1469	597644.0898	1852676.1770	-916.10
2446	1470	597780.4051	1852703.3580	-915.10
2447	1471	597911.3853	1852731.6220	-914.10
2448	1472	598047.6999	1852758.8060	-913.80
2449	1473	598188.2676	1852788.2220	-911.30
2450	1474	598320.3128	1852816.4940	-911.45
2451	1475	598457.6821	1852845.8980	-912.20
2452	1476	598596.1222	1852874.2010	-909.60
2453	1477	598732.4198	1852904.7080	-908.40
2454	1478	598865.5348	1852931.8820	-908.25
2455	1479	599001.8472	1852959.0720	-907.80
2456	1480	599139.2149	1852988.4800	-906.90
2457	1481	599271.2631	1853015.6510	-904.80
2458	1482	599408.6353	1853043.9550	-902.90
2459	1483	599544.9361	1853073.3610	-902.90
2460	1484	599679.1100	1853101.6510	-901.90
2461	1485	599816.4865	1853128.8510	-900.50
2462	1486	599952.7863	1853158.2600	-898.65

FFID	Shot #	UTM Easting (m)	UTM Northing (m)	Depth (m)
2463	1487	600088.0199	1853187.6640	-897.20
2464	1488	600225.3850	1853217.0800	-896.60
2465	1489	600357.4307	1853244.2580	-895.10
2466	1490	600494.8004	1853272.5690	-893.80
2467	1491	600625.7744	1853300.8500	-893.15
2468	1492	600761.0169	1853328.0460	-891.80
2469	1493	600902.6439	1853357.4870	-887.90
2470	1494	601037.8753	1853386.8970	-887.30
2471	1495	601173.1116	1853415.2020	-887.05
2472	1496	601310.4740	1853444.6250	-886.80
2473	1497	601445.7044	1853474.0380	-885.60
2474	1498	601578.8133	1853501.2300	-885.30
2475	1499	601710.8507	1853529.5230	-882.50
2476	1500	601851.4148	1853557.8580	-880.70
2477	1501	601988.7757	1853587.2850	-878.60
2478	1502	602122.9439	1853615.5920	-876.80
2479	1503	602260.3041	1853645.0210	-875.80
2480	1504	602398.7352	1853673.3490	-874.45
2481	1505	602529.7048	1853701.6430	-872.65
2482	1506	602667.0747	1853728.8620	-870.70
2483	1507	602804.4336	1853758.2940	-868.60
2484	1508	602939.6658	1853786.6110	-868.25
2485	1509	603078.0845	1853817.1570	-867.90
2486	1510	603211.1843	1853845.4650	-865.50
2487	1511	603347.4760	1853874.8960	-864.80
2488	1512	603483.7728	1853903.2210	-863.30
2489	1513	603620.0693	1853931.5480	-861.90
2490	1514	603752.1074	1853958.7480	-860.20
2491	1515	603891.5954	1853988.1980	-857.80
2492	1516	604015.1168	1854013.1450	-857.15
2493	1517	604140.7806	1854035.8910	-856.50
2494	1518	604270.7404	1854052.0200	-856.00
2495	1519	604394.3429	1854060.3740	-853.80
2496	1520	604532.9386	1854054.4200	-852.90

APPENDIX D: PROCESSING

INTRODUCTION

Processing of the SEA-CALIPSO data required the understanding of the SEA-CALIPSO experiment geometry to understand the location of all instruments in the experiment, the topography of Montserrat, and the bathymetry of the ocean floor around the island (Fig. 11). Lack of near-source data produced a challenge for processing as many attempts to remove multiples were unsuccessful. Standard processing techniques were used to create 6 images of the eastern oceanic crust near Montserrat.

SEGY SHOT FILES

SEGY shot gathers were chosen by analyzing times when the ship was directly inline (parallel and co-parallel) with the Silver Hills RT-125a's (Figure 10). This was accomplished by studying a video showing the shiptrack of the SEA-CALIPSO experiment (CD insert). Times were written down when the ship was in alignment with the RT125a's (Table 15). The locations of these shot files was located and plotted using the program GMT (Wessel and Smith, 2006) which was used to ensure that the chosen shots were parallel and co-parallel with the Silver Hills Texans (Figure 10). SEGY shot gathers were input into ProMAX®, for reflection processing. Within the input flow, a mean trace DC removal was used to remove electronic instrument noise.

GEOMETRY

Once the Silver Hills Ship track gathers were entered, a geometry extraction was preformed to load the file headers. In the case of the SEA-CALIPSO data, this was not useful, as the headers did not contain any information. In order to remediate this problem, a geometry load was preformed.

Geometry load for the 10 Silver hills profiles consisted of geometry file creation, which contained the location of the shots offshore, and the RT125a's onshore (see Tables 3-13, Appendix C). These files were input into ProMAX® along with the following information: Nominal Receiver Spacing = 100 m, Nominal Source Spacing = 125 m, first live station =1, last live station = 63. Receiver information was imported from tables and placed into the receiver spreadsheet. Source information was imported from tables and placed into the sources spreadsheet. The pattern spreadsheet, which identifies how the receiver, source, and setup spreadsheets are used, was filled in with the following information: Pattern = 1, minimum channel =1, maximum channel = 63, channel increment =1, receiver minimum = 1, receiver maximum = 63, receiver increment =1. Following the input of this information, the data was binned and checked to ensure locations were input correctly.

Once the data was binned, geometry load was preformed which imported the spreadsheet information into the headers, along with information automatically calculated such as CMP locations. The geometry of the experiment provided a fold of 63.

TRACE EDITING

Shot gathers were created using the inline sort tool to asses the quality of the reflection data. Traces, which contained large amounts of noise, or were not recording properly (Figures 12 & 13) were muted using trace kill.

AUTOMATIC GAIN CONTROL

An automatic gain control (AGC) was applied to the data using a 500 ms root mean square gain window to adjust amplitudes.

STATICS

Elevation statics were applied to the data to account for elevation differences between receivers and shots. This flow calculated the shift traces needed in order to represent receivers and shots as though they were at the same elevation. Static shift was accomplished after the geometry load and placed a final datum at sea level. The replacement velocity 4500 m/s was chosen because it represents the combined velocity of the water column (1500 m/s) and average sedimentary velocities (3000 m/s). Following the calculation apply statics was used to import the data.

VELOCITY DEVELOPMENT

The development of a velocity profile is necessary to apply a normal move-out (NMO), which aligns (CMP's) and stacked. The NMO takes advantage of constructive and destructive interference.

SEMBLANCE

Semblance was attempted with the Silver Hills data, but failed due to the geometry of the SEA-CALIPSO experiment, the volcanic material, and the lack of CMP's. The failure of semblance lead to the creation of an interval velocity model.

INTERVAL VELOCITY ANALYSIS

An interval velocity model was developed (Table 16) using information from available literature on the Caribbean crust (Boynton et al., 1979; Christeson et al., 2008). Looking at the 6 Silver Hills eastern profiles and modifying velocities to align reflections refined this model. The final velocity model (Table 16) was a result of the combined literature review and the results of the modified velocity model.

NORMAL MOVE-OUT (NMO)

The NMO used the interval velocity that was developed to flatten reflections within the Silver Hills profiles. This process prepares the data for stacking.

STACKING

Once the NMO was applied the data was stacked, which takes advantage of constructive and destructive interference. This allows for reflections to add constructively and noise to combine destructively.

BANDPASS FILTERING

Different Butterworth bandpass filters were used to remove frequencies, which were not useful within the SEA-CALIPSO data. These filters are designed with 4 frequencies, f1-f2-f3-f4. Frequency 1 is the cut off frequency, everything below this

frequency is cut from the data, frequency 2 is the first frequency not tapered. The slope between 1 and 2 defines how tapering of frequencies are performed. If frequencies were cut out suddenly, residual effects would result within the data. Frequency 3 is the last frequency to be un-tapered. Frequency 4 is the cut off frequency; all frequencies after this value are removed completely from the data. It was decided after reviewing several combinations to use the 4-8-20-30 filter.

Butterworth Filters
4-8-30-40
4-8-20-30
4-8-25-35
4-8-15-35
4-8-25-40
4-8-10-15

LINEAR MOVE-OUT (LMO)

An attempt to perform a LMO on the Silver Hills data to shift suspected refractions was conducted. A velocity of 3,000 m/s was used for offsets of 1 km, and a velocity of 6,000 m/s was used for offsets of 2 km. This attempt failed to move any refraction, leaving the assumption that there are no refractions within the data. A second attempt at LMO was conducted with the reduced velocity of 2300 m/s. This attempt met with the same results as the first.

PARABOLIC RADON TRANSFORM

A parabolic radon transform was attempted in order to remove multiples from the data. The parabolic transform allows for the mapping of reflections, and their multiples to points within the parabolic tau-p domain. Filters are then used to remove multiples from this domain and an inverse transform is used. Due to lack of near-source data, the multiples and reflections mapped into the parabolic Tau-p domain, are indistinguishable from noise.

DECONVOLUTION

Deconvolution using Adaptive Deconvolution and Spiking/Predictive Deconvolution were conducted. Each Silver Hills East line was processed separately in order to maximize the effectiveness of the deconvolution. Deconvolution is used to remove predictable multiples.

Profile	Operator Length (ms)	Predictor Length (ms)	Percent White Noise	Notch Filter (Hz)	Butterworth Filter (Hz)
SH 540	294	160	0.1	5	2-4-30-45
SH 550	294	160	0.1	5	2-4-30-45
SH 551	192	160	0.1	5	2-4-30-45
SH 560	192	160	0.1	5	2-4-30-45
SH 561	192	200	0.1	5	2-4-30-45
SH 562	294	160	0.1	5	2-4-30-45

Table 14: Deconvolution parameters used for the six Silver Hills lines.

DIP MOVE-OUT (DMO)

Dipping reflections found in Silver Hills lines 551, 561, and 562 were performed to ensure they were not residual processing effects. A DMO was attempted in order to remove any aliasing found within the data. The DMO produced aliasing within the Silver Hills data and was therefore abandoned. Frequencies investigated within the DMO were, 2-80 Hz, 0-80 Hz, and 0-45 Hz.

F-K FILTER

A frequency-wave number filter was attempted to remove noise within the data. This filter was designed using 0 to 0.0027/m wave number, and a 16-27 Hz bandwidth. This filter failed to produce a change within the reflection images, and was not used.

MIGRATION

A Kirchhoff time migration was attempted using a CMP interval of 50 m, maximum frequency of 45 Hz, aperture 0, and maximum dip 90°. The migration failed to work on the Silver Hills data due to the assumption of zero-offset stacking.

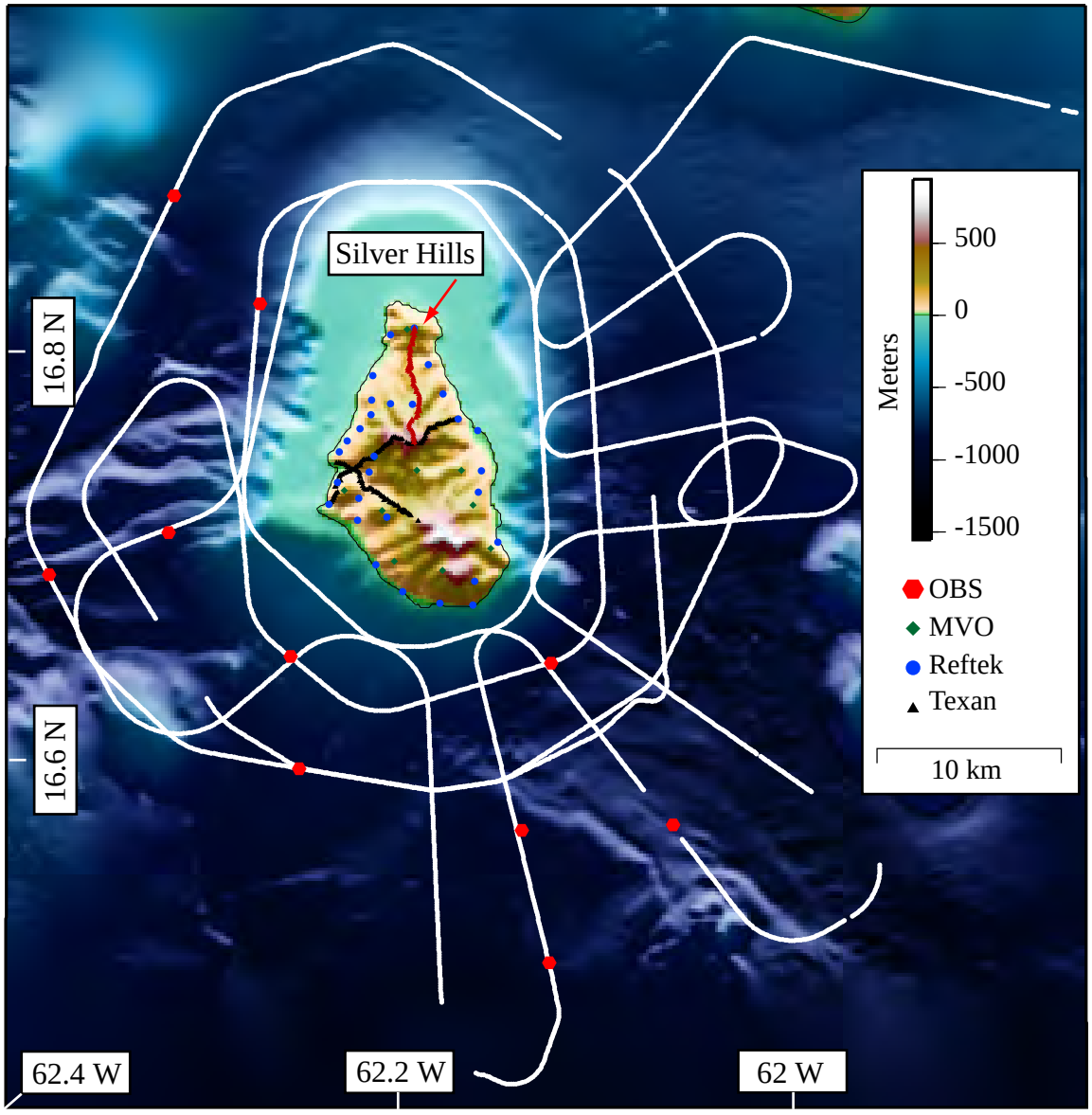

Figure 11: Shiptrack and instrument location for the SEA-CALIPSO experiment. Ocean bottom seismometers (OBS), red hexigons, Montserrat Volcano Observatory instruments (MVO), green diamonds, RT130 3 component geophones, blue circles, and RT125a single component geophones (texans), black triangles. Silver Hills line, red triangles, running north to south, Centre Hills line running west to east, Garibaldi line running southwest to northeast and Belham Valley line running from northwest to southeast.

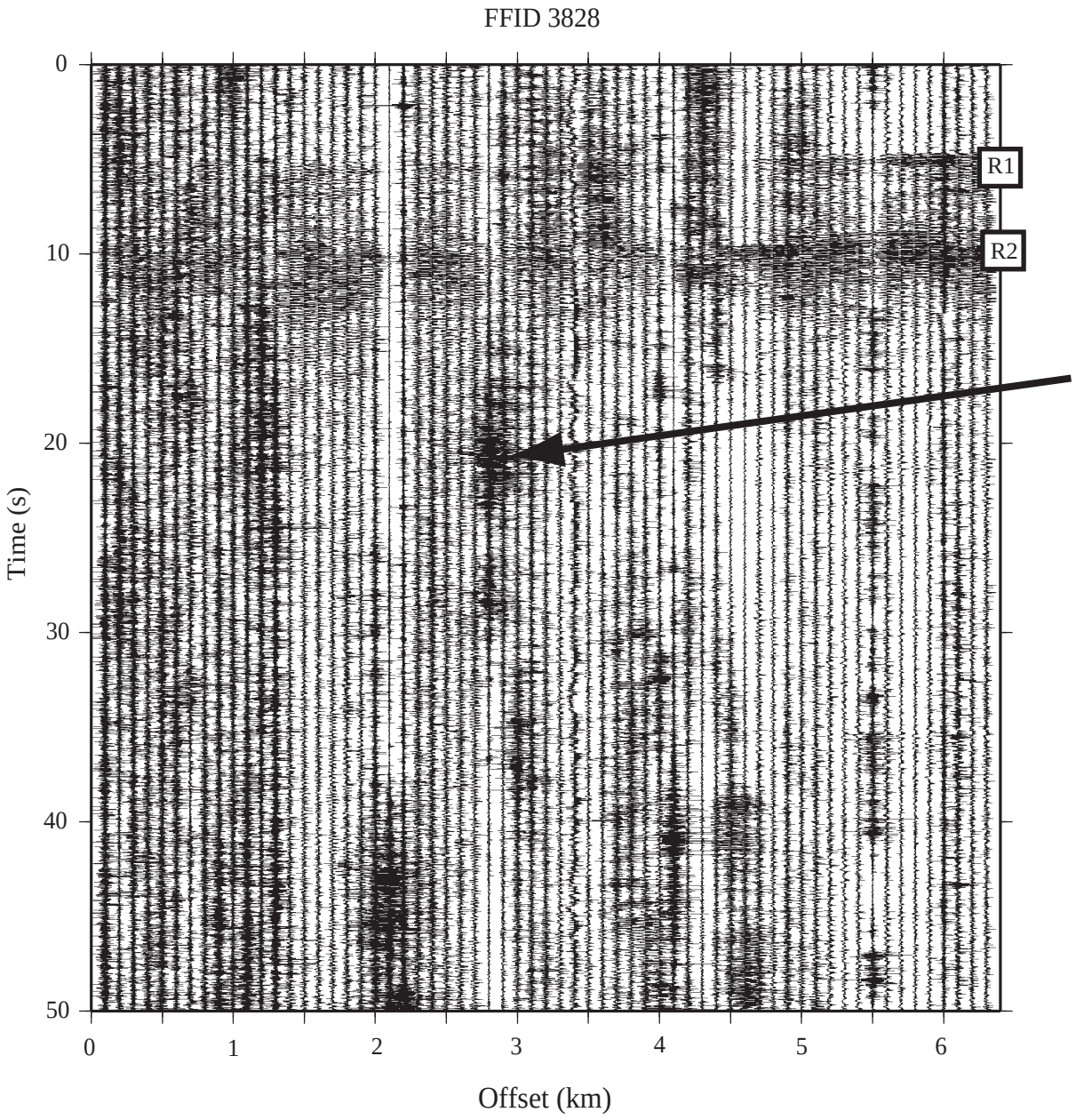

Figure 12: Shot gather of shot number 3828 on SH_560. Two reflectors appear within the first 13 s (R1, R2). Poor quality of reflection data, arrow, appears throughout all of the Silver Hills data.

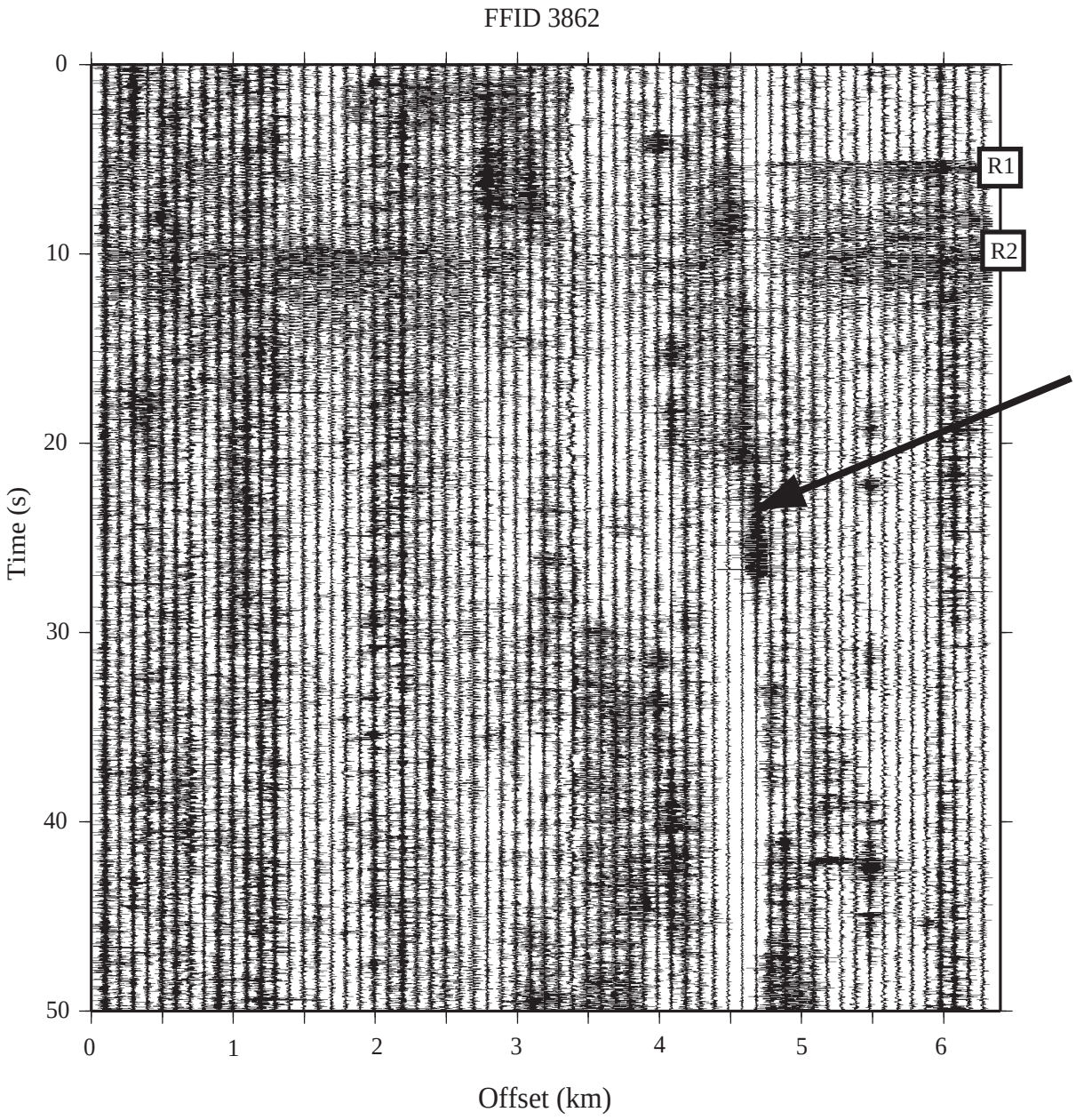

Figure 13: Shot gather of shot number 3862 on SH_560. Two reflectors appear within the first 13 s (R1, R2). Poor quality of reflection data, arrow, appears throughout all of the Silver Hills data.

Table 15: Silver Hills Shot Times, Figure 10

Shiptrack	Begin Time Day:Hour:Min	End Time Day:Hour:Min
SH_500	352:22:45	353:01:25
SH_510	353:09:07	353:10:01
SH_520	354:00:53	354:01:47
SH_530	352:07:18	352:08:11
SH_540	351:19:09	351:20:03
SH_550	354:05:10	354:06:05
SH_551	352:11:14	352:12:32
SH_560	353:16:09	353:17:02
SH_561	352:13:44	352:15:05
SH_562	352:15:34	352:16:48

Table 16: Interval Velocity Model for Silver Hills Lines, Reflectors shown (pink squares) and highlighted in table (yellow).

TWTT (s)	Velocity (km/s)	Depth (m)
0	1.5	0
0.1	1.5	0.075
0.2	1.5	0.15
0.3	1.5	0.225
0.4	1.5	0.3
0.5	1.5	0.375
0.6	1.5	0.45
0.7	1.5	0.525
0.8	1.5	0.6
0.9	1.5	0.675
1	1.5	0.75
1.1	1.5	0.825
1.2	1.5	0.9
1.3	1.5	0.975
1.4	1.5	1.05
1.5	3.3	1.215
1.6	3.3	1.38
1.7	3.3	1.545
1.8	3.3	1.71
1.9	3.3	1.875
2	3.3	2.04
2.1	3.3	2.205
2.2	3.3	2.37
2.3	3.3	2.535
2.4	3.3	2.7
2.5	3.3	2.865
2.6	3.3	3.03
2.7	3.3	3.195
2.8	3.3	3.36
2.9	3.3	3.525
3	6	3.825
3.1	6	4.125
3.2	6	4.425
3.3	6	4.725
3.4	6	5.025
3.5	6	5.325
3.6	6	5.625
3.7	6	5.925
3.8	6	6.225

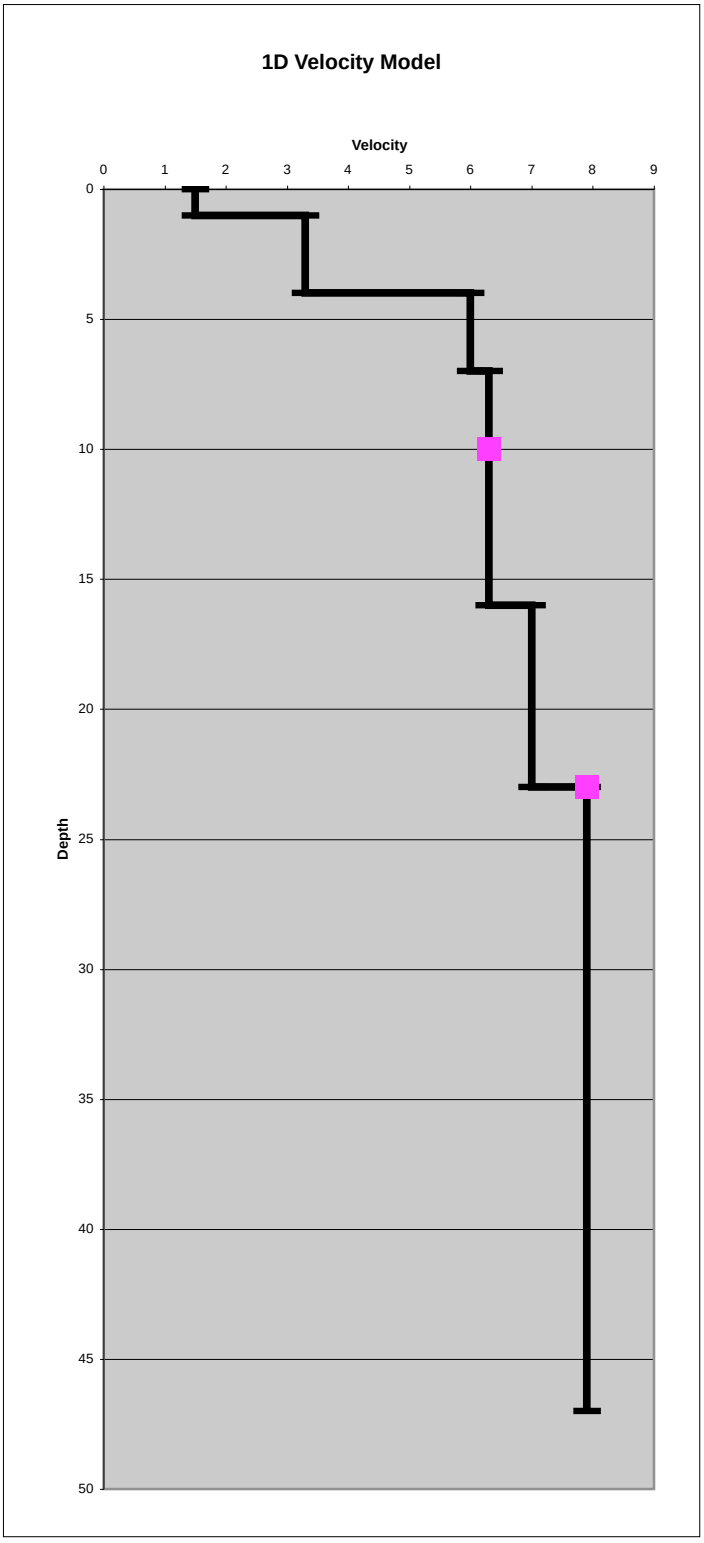

TWTT (s)	Velocity (km/s)	Depth (m)
3.9	6	6.525
4	6.3	6.84
4.1	6.3	7.155
4.2	6.3	7.47
4.3	6.3	7.785
4.4	6.3	8.1
4.5	6.3	8.415
4.6	6.3	8.73
4.7	6.3	9.045
4.8	6.3	9.36
4.9	6.3	9.675
5	6.3	9.99
5.1	6.3	10.305
5.2	6.3	10.62
5.3	6.3	10.935
5.4	6.3	11.25
5.5	6.3	11.565
5.6	6.3	11.88
5.7	6.3	12.195
5.8	6.3	12.51
5.9	6.3	12.825
6	6.3	13.14
6.1	6.3	13.455
6.2	6.3	13.77
6.3	6.3	14.085
6.4	6.3	14.4
6.5	6.3	14.715
6.6	6.3	15.03
6.7	6.3	15.345
6.8	6.3	15.66
6.9	6.3	15.975
7	7	16.325
7.1	7	16.675
7.2	7	17.025
7.3	7	17.375
7.4	7	17.725
7.5	7	18.075
7.6	7	18.425
7.7	7	18.775
7.8	7	19.125
7.9	7	19.475

TWTT (s)	Velocity (km/s)	Depth (m)
8	7	19.825
8.1	7	20.175
8.2	7	20.525
8.3	7	20.875
8.4	7	21.225
8.5	7	21.575
8.6	7	21.925
8.7	7	22.275
8.8	7	22.625
8.9	7	22.975
9	7.9	23.37
9.1	7.9	23.765
9.2	7.9	24.16
9.3	7.9	24.555
9.4	7.9	24.95
9.5	7.9	25.345
9.6	7.9	25.74
9.7	7.9	26.135
9.8	7.9	26.53
9.9	7.9	26.925
10	7.9	27.32
10.1	7.9	27.715
10.2	7.9	28.11
10.3	7.9	28.505
10.4	7.9	28.9
10.5	7.9	29.295
10.6	7.9	29.69
10.7	7.9	30.085
10.8	7.9	30.48
10.9	7.9	30.875
11	7.9	31.27
11.1	7.9	31.665
11.2	7.9	32.06
11.3	7.9	32.455
11.4	7.9	32.85
11.5	7.9	33.245
11.6	7.9	33.64
11.7	7.9	34.035
11.8	7.9	34.43
11.9	7.9	34.825
12	7.9	35.22

TWTT (s)	Velocity (km/s)	Depth (m)
12.1	7.9	35.615
12.2	7.9	36.01
12.3	7.9	36.405
12.4	7.9	36.8
12.5	7.9	37.195
12.6	7.9	37.59
12.7	7.9	37.985
12.8	7.9	38.38
12.9	7.9	38.775
13	7.9	39.17
13.1	7.9	39.565
13.2	7.9	39.96
13.3	7.9	40.355
13.4	7.9	40.75
13.5	7.9	41.145
13.6	7.9	41.54
13.7	7.9	41.935
13.8	7.9	42.33
13.9	7.9	42.725
14	7.9	43.12
14.1	7.9	43.515
14.2	7.9	43.91
14.3	7.9	44.305
14.4	7.9	44.7
14.5	7.9	45.095
14.6	7.9	45.49
14.7	7.9	45.885
14.8	7.9	46.28
14.9	7.9	46.675
15	7.9	47.07

APPENDIX E: ADDITIONAL SILVER HILLS PROFILES

ADDITIONAL SILVER HILLS PROFILES

Ten profiles were created and investigated using the Silver Hills transects (Fig. 10). Brute stacks were created by applying the geometry, elevation static shift, CMP sort, and an NMO using the interval velocity (Table 16). The brute stacks were studied to identify the best seismic profiles for further processing. Of the 10 Silver Hills lines, the Silver Hills east lines were chosen for complete processing (Fig. 14).

The 4 Silver Hills profiles that were not processed further are shown in figures 15-18. The 6 Silver Hills eastern profiles were completely processed; using the processes listed in Table 1 and discussed in Appendix D, are shown in figures 3, 19-23.

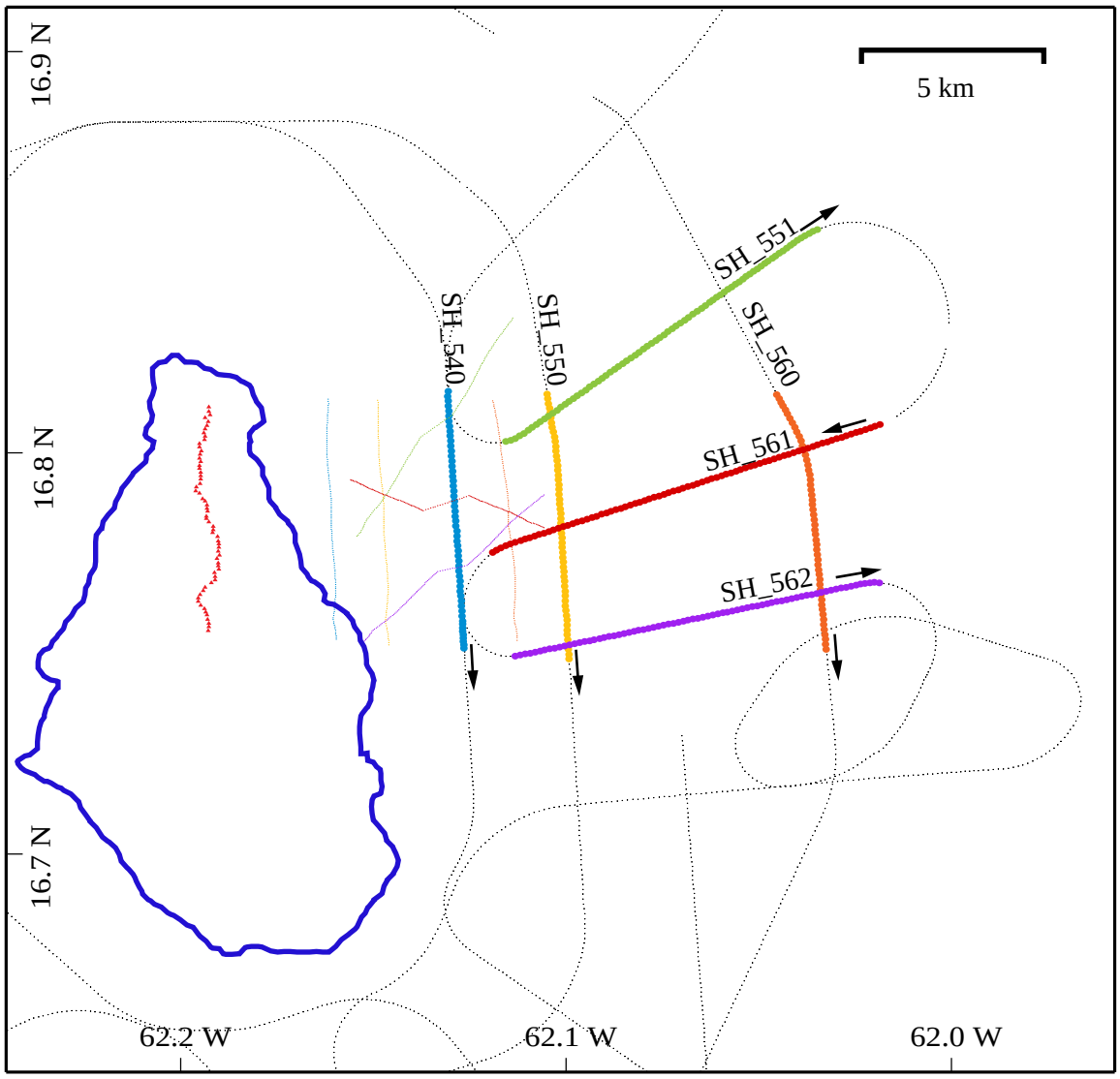

Figure 14: Silver Hills east lines, SH_540 (light blue), SH_550 (gold), and SH_560 (orange) are parallel to the Silver Hills recorders (red triangles). Silver Hills east lines SH_551 (green), SH_561 (red), and SH_562 (purple) are perpendicular to the Silver Hills recorders. Common midpoints (CMPs), plotted in the same color as the shiptracks, show the location of reflection images.

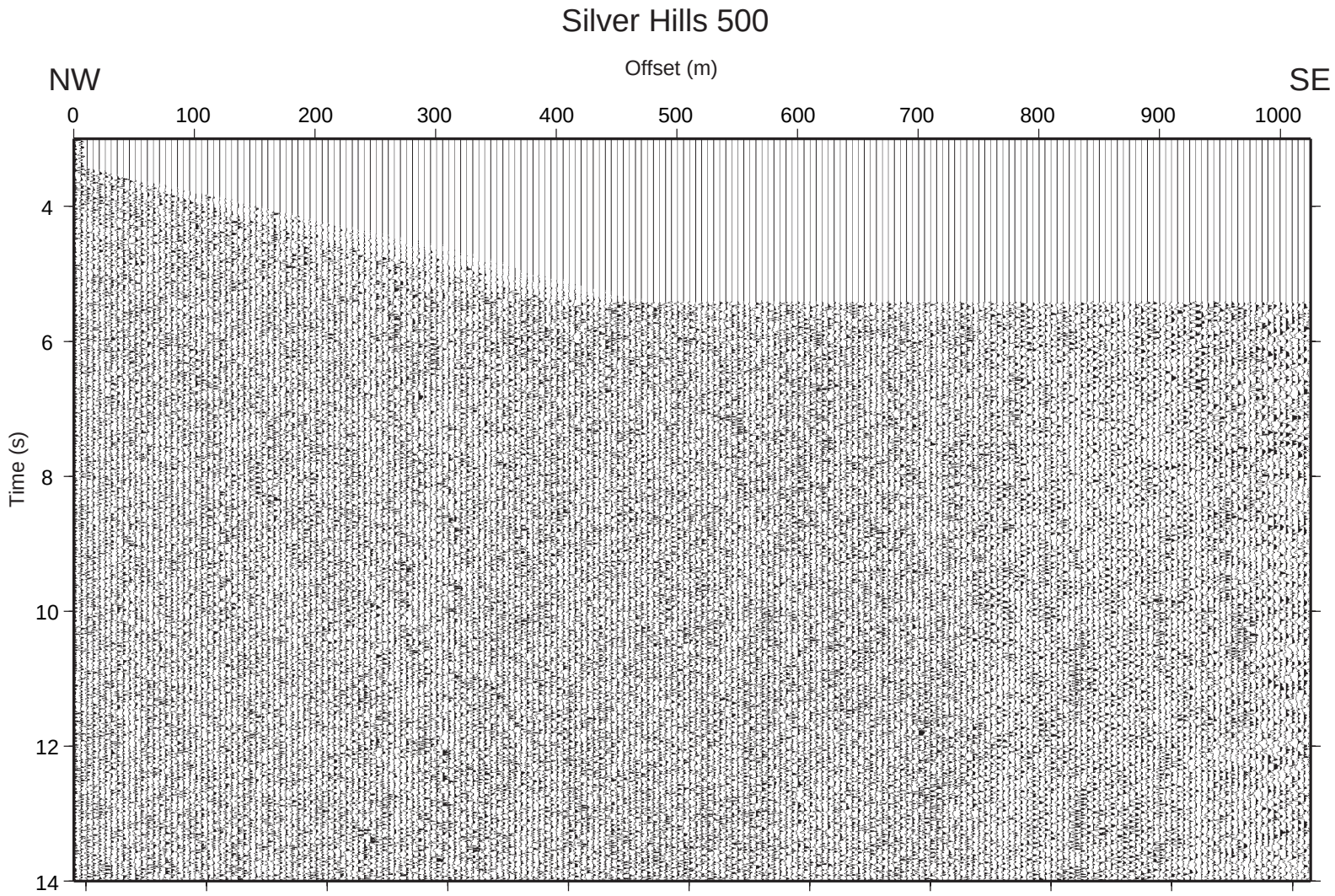

Figure 15: Brute Stack of Silver Hills 500

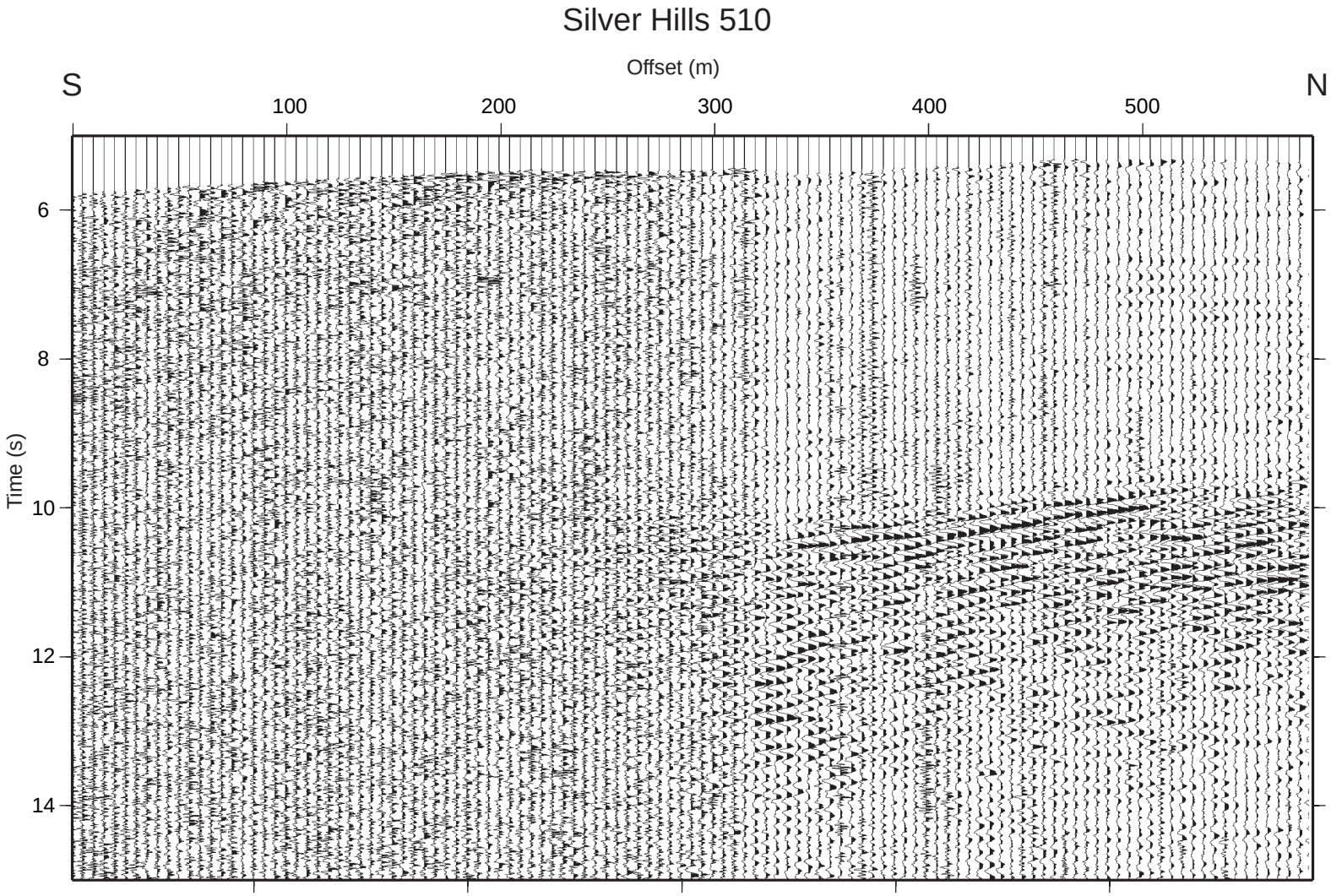

Figure 16: Brute Stack of Silver Hills 510

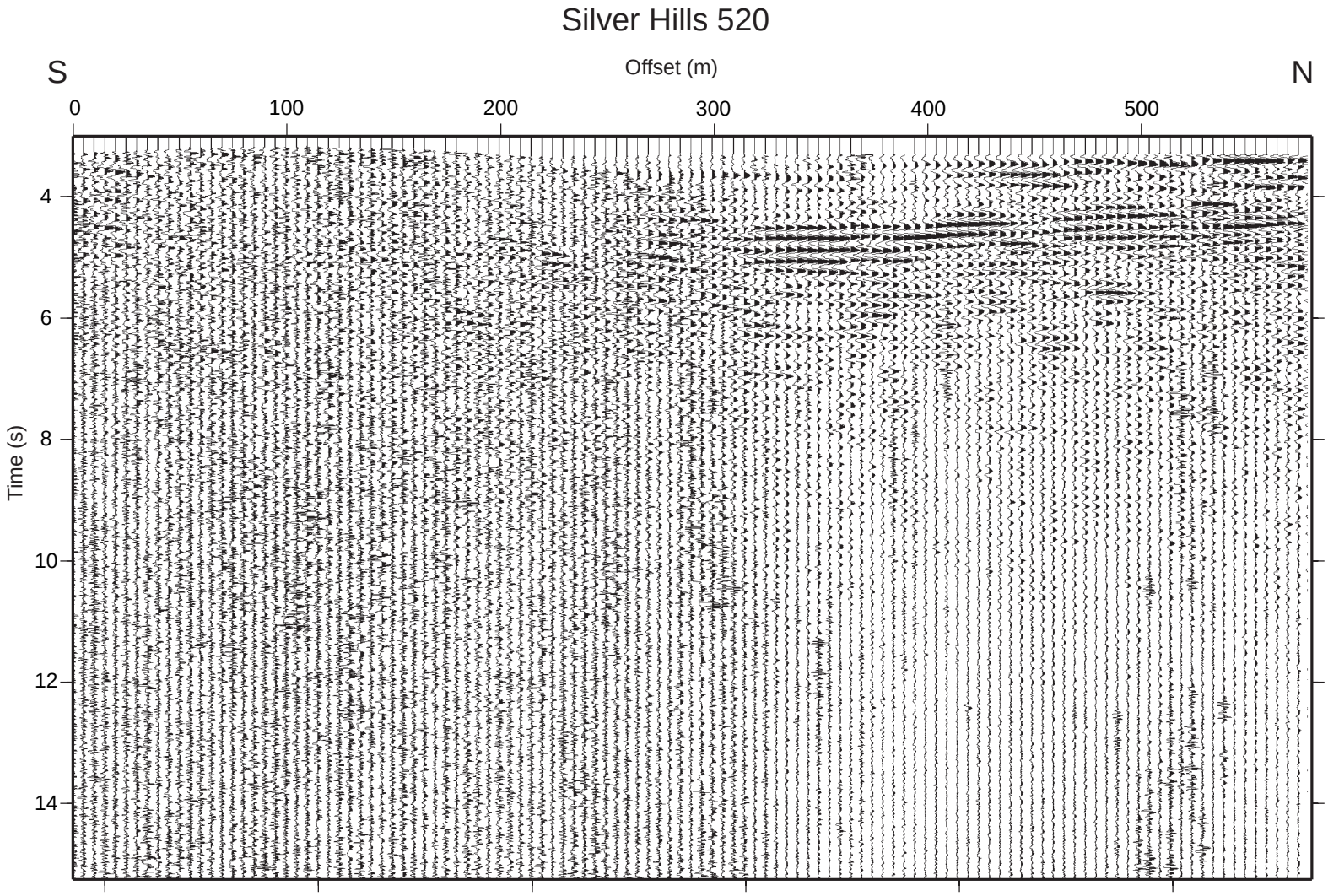

Figure 17: Brute Stack of Silver Hills 520

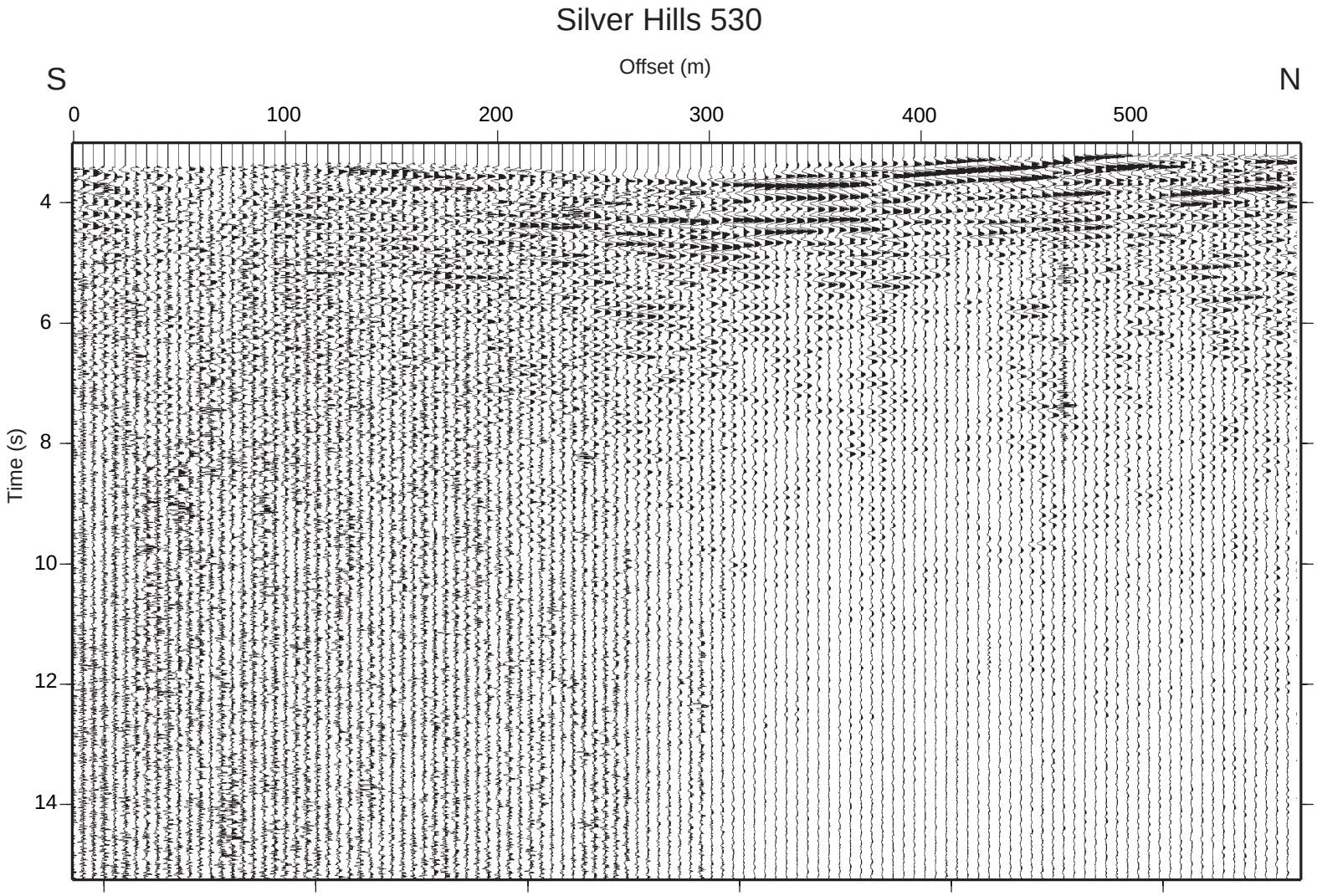

Figure 18: Brute Stack of Silver Hills 530

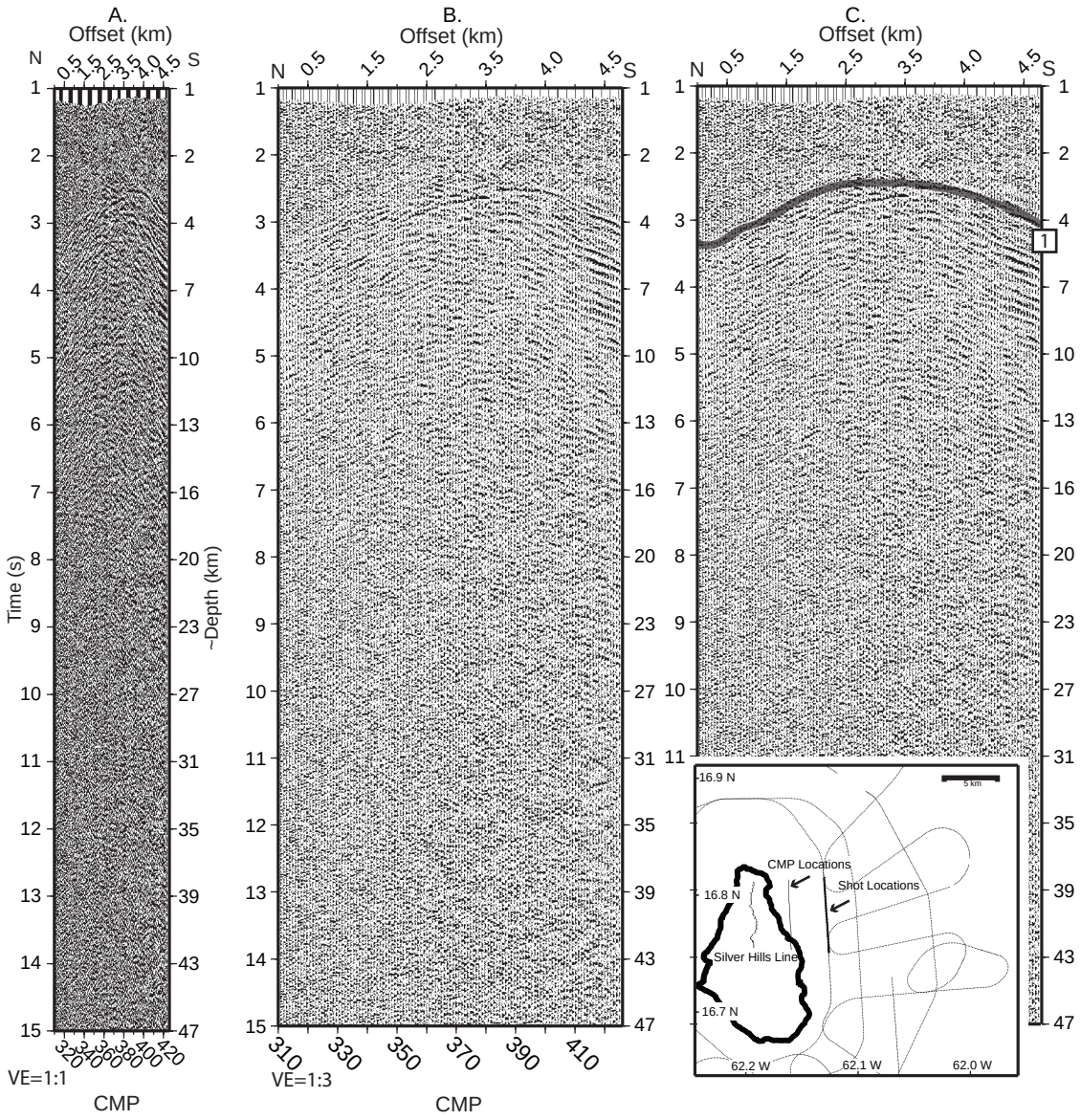

Figure 19: The processed Silver Hills 540 reflection stack that is approximately 3 km offshore Montserrat (see inset) is displayed in 3 panes (a, b, c). (a) Displayed data with no vertical exaggeration has one reflection appearing at ~ 3 s (depth ~4 km). (b) Horizontal exaggeration 1:3. (c) Interpreted section with Reflector 1 at 3 s

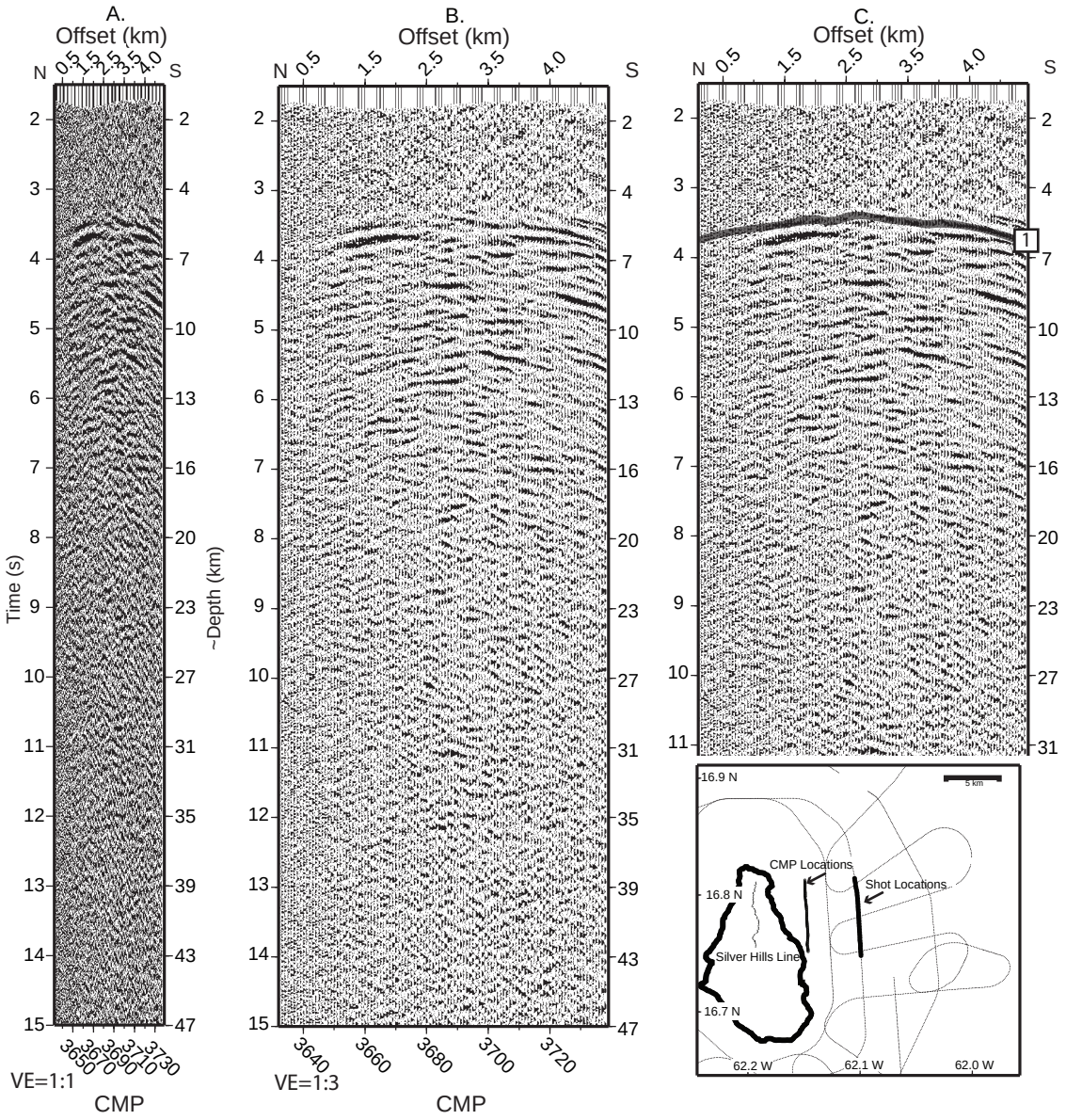

Figure 20: The processed Silver Hills 550 reflection stack that is approximately 5 km offshore Montserrat (see inset) is displayed in 3 panels (a, b, c). (a) Displayed data with no vertical exaggeration has one reflection appearing at ~ 4s (depth ~6 km). (b) Horizontal exaggeration 1:3. (c) Interpreted section with Reflector 1 at 4 s.

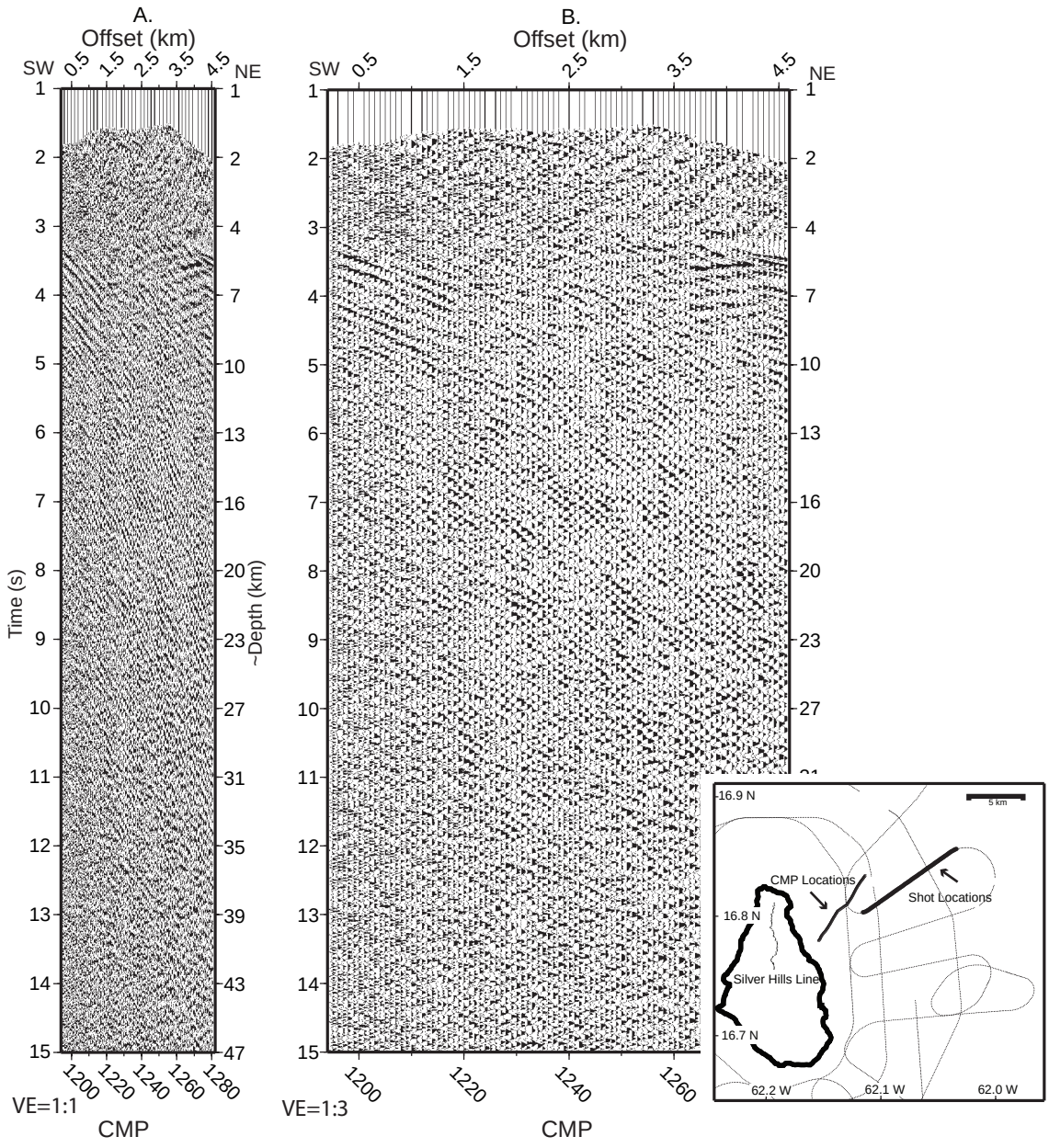

Figure 21: Processed Silver Hills 551 reflection stack. Stack produced through processing described in Table 1.

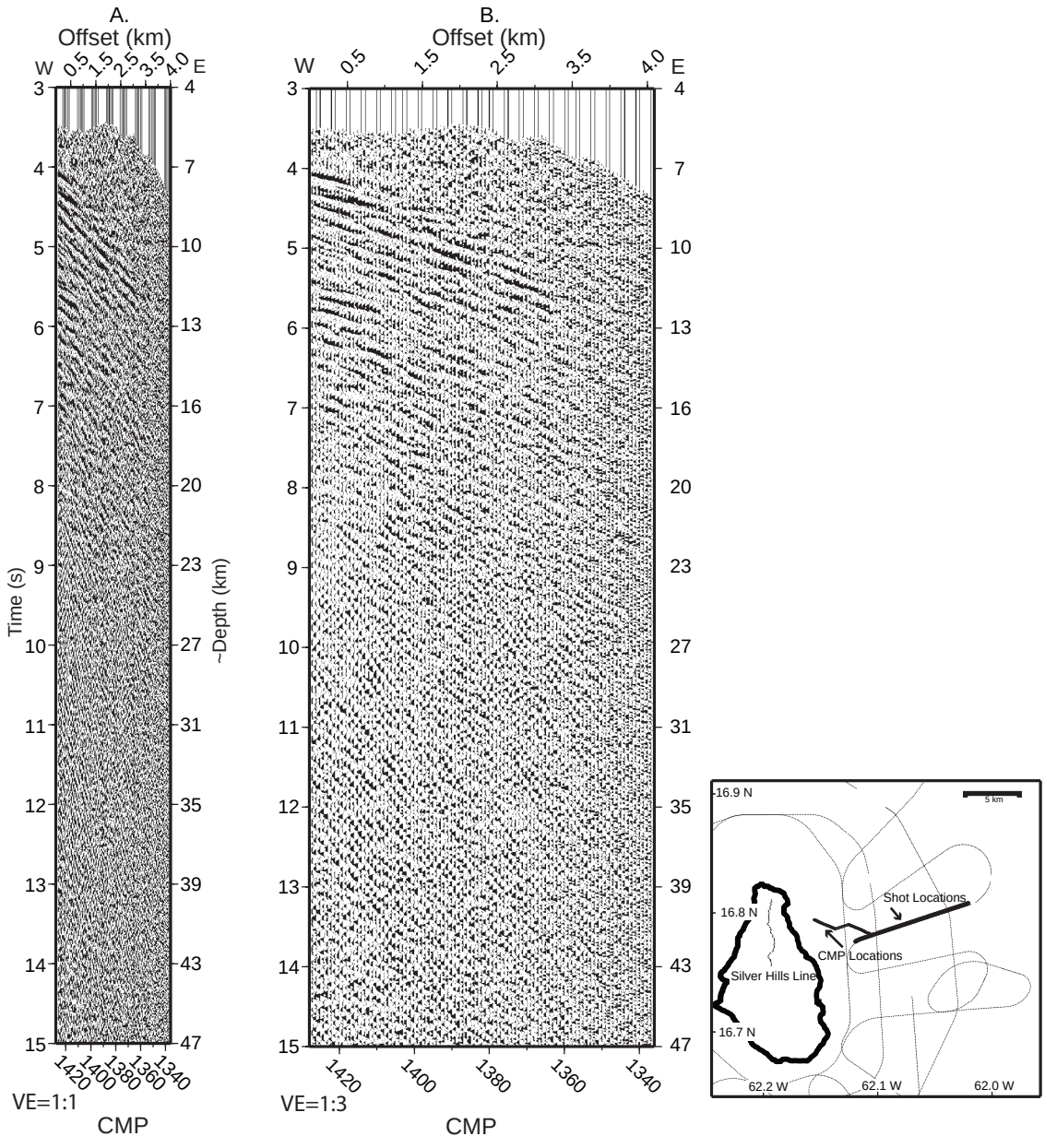

Figure 22: Processed Silver Hills 561 reflection stack. Stack produced through processing described in Table 1

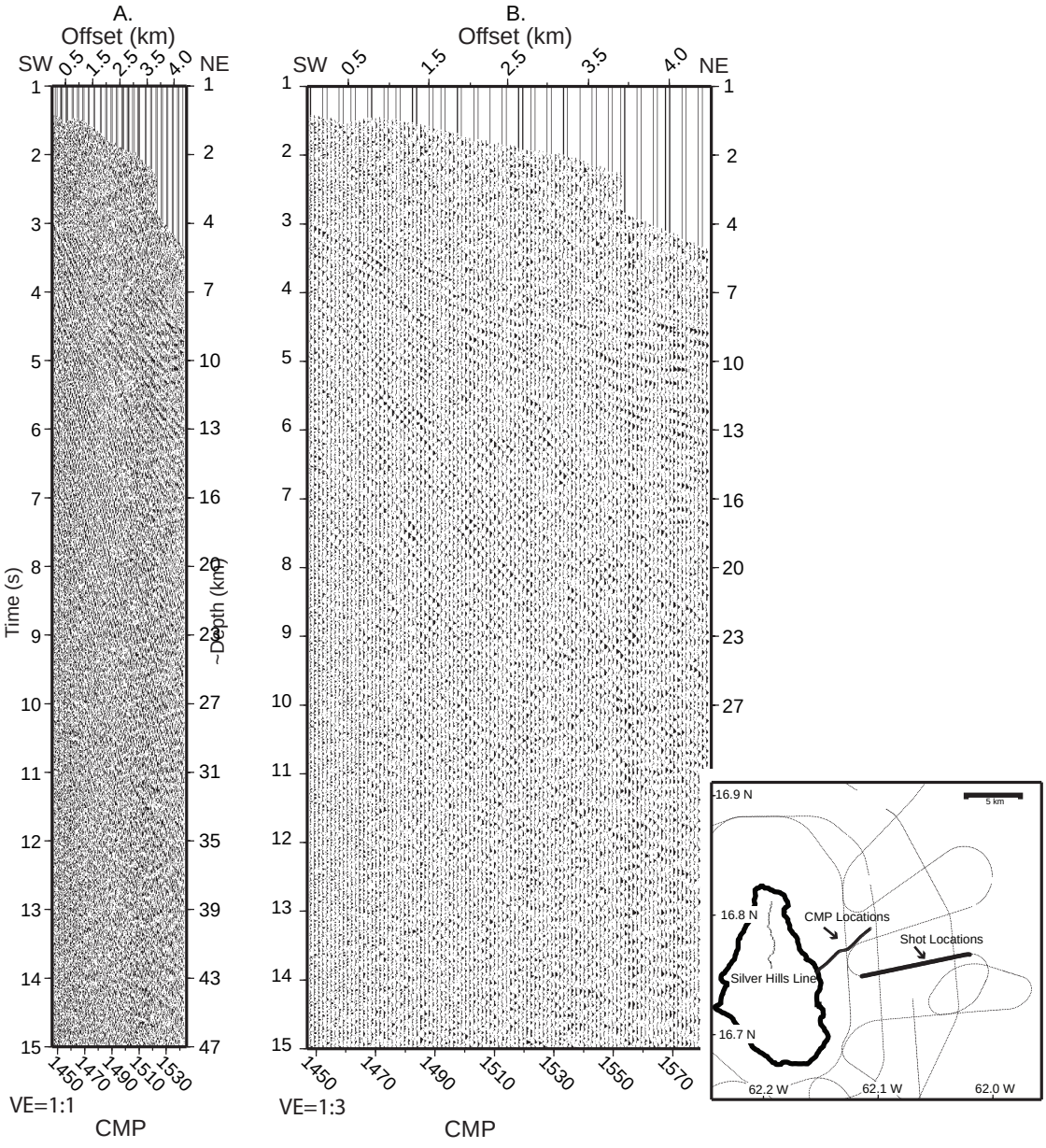

Figure 23: Processed Silver Hills 562 reflection stack. Stack produced through procesing described in Table 1